J Geod (2011) 85:819–843
DOI 10.1007/s00190-011-0467-x

ORIGINAL ARTICLE

First GOCE gravity field models derived by three different approaches

Roland Pail · Sean Bruinsma · Federica Migliaccio · Christoph Förste · Helmut Goiginger · Wolf-Dieter Schuh · Eduard Höck · Mirko Reguzzoni · Jan Martin Brockmann · Oleg Abrikosov · Martin Veicherts · Thomas Fecher · Reinhard Mayrhofer · Ina Krasbutter · Fernando Sansò · Carl Christian Tscherning

Received: 25 September 2010 / Accepted: 25 March 2011

Abstract Three gravity field models, parameterized in terms of spherical harmonic coefficients, have been computed from 71 days of GOCE (Gravity field and steady-state Ocean Circulation Explorer) orbit and gradiometer data by applying independent gravity field processing methods. These gravity models are one major output of the Euro-

R. Pail (✉) · T. Fecher
Institute of Astronomical and Physical Geodesy, TU München, Arcisstraße 21, 80333 Munich, Germany
e-mail: pail@bv.tum.de

T. Fecher
e-mail: fecher@bv.tu-muenchen.de

S. Bruinsma
Department of Terrestrial and Planetary Geodesy, CNES-DCT/SI/GS, 18, avenue E. Belin, 31401 Toulouse Cedex 9, France
e-mail: sean.bruinsma@cnes.fr

F. Migliaccio · M. Reguzzoni
Politecnico di Milano, DIIAR-Sez. Rilevamento, Piazza Leonardo da Vinci 32, 20133 Milan, Italy
e-mail: federica.migliaccio@polimi.it

M. Reguzzoni
e-mail: mirko@geomatica.como.polimi.it

C. Förste · O. Abrikosov
Department 1: Geodesy and Remote Sensing, Section 1.2: Global Geomonitoring and Gravity Field, Helmholtz Centre Potsdam, GFZ German Research Centre for Geosciences, Telegrafenberg A17, 14473 Potsdam, Germany
e-mail: foer@gfz-potsdam.de

O. Abrikosov
e-mail: abrik@gfz-potsdam.de

H. Goiginger · R. Mayrhofer
Institute of Theoretical Geodesy and Satellite Geodesy, Graz University of Technology, Steyrergasse 30, 8010 Graz, Austria
e-mail: h.goiginger@tugraz.at

R. Mayrhofer
e-mail: reinhard.mayrhofer@tugraz.at

W.-D. Schuh · J. M. Brockmann · I. Krasbutter
Institute of Geodesy and Geoinformation, University of Bonn, Nussallee 17, 53115 Bonn, Germany
e-mail: schuh@uni-bonn.de

J. M. Brockmann
e-mail: brockmann@geod.uni-bonn.de

I. Krasbutter
e-mail: Ina.krasbutter@geod.uni-bonn.de

E. Höck
Department of Satellite Geodesy, Space Research Institute, Austrian Academy of Sciences, Schmiedlstraße 6, 8042 Graz, Austria
e-mail: hoeck@geomatics.tu-graz.ac.at

O. Abrikosov
Münchner Str. 20, c/o DLR Oberpfaffenhofen, 82234 Wessling, Germany

M. Veicherts · C. C. Tscherning
Niels Bohr Institute, University of Copenhagen, Juliane Maries Vej 30, 2100 Copenhagen, Denmark
e-mail: mave@gfy.ku.dk

C. C. Tscherning
e-mail: cct@gfy.ku.dk

F. Sansò
Politecnico di Milano, Polo Regionale di Como, via Valleggio 11, 22100 Como, Italy
e-mail: fernando.sanso@polimi.it

pean Space Agency (ESA) project GOCE High-level Processing Facility (HPF). The processing philosophies and architectures of these three complementary methods are presented and discussed, emphasizing the specific features of the three approaches. The resulting GOCE gravity field models, representing the first models containing the novel measurement type of gravity gradiometry ever computed, are analysed and assessed in detail. Together with the coefficient estimates, full variance-covariance matrices provide error information about the coefficient solutions. A comparison with state-of-the-art GRACE and combined gravity field models reveals the additional contribution of GOCE based on only 71 days of data. Compared with combined gravity field models, large deviations appear in regions where the terrestrial gravity data are known to be of low accuracy. The GOCE performance, assessed against the GRACE-only model ITG-Grace2010s, becomes superior at degree 150, and beyond. GOCE provides significant additional information of the global Earth gravity field, with an accuracy of the 2-month GOCE gravity field models of 10 cm in terms of geoid heights, and 3 mGal in terms of gravity anomalies, globally at a resolution of 100 km (degree/order 200).

Keywords Gravity field · GOCE · Gradiometry · GPS · Spherical harmonics · Global gravity model

1 Introduction

Dedicated satellite gravity missions have revolutionized our knowledge about the global Earth gravity field. The CHallenging Minisatellite Payload (CHAMP; Reigber et al. 2002) mission, launched on 15 July 2000, constituted the first gravity field mission carrying a GPS receiver with continuous 3-D tracking capability and a precise accelerometer to measure the non-gravitational forces. One of the first models developed with only 6 months of CHAMP data improved the GRIM5-S1 model (Biancale et al. 2000) by almost one order of magnitude up to degree 35 (Reigber et al. 2003). The Gravity Recovery and Climate Experiment (GRACE; Tapley et al. 2004) twin satellite mission, launched on 17 March 2002, is the second dedicated gravity field mission. Models inferred from the GRACE Ka-band ranging data as well as the continuous 3-D tracking by means of GPS gained approximately two orders of magnitude in accuracy (1 cm geoid error at degree 100) as compared with GRIM5-S1. State-of-the-art models determined with five or more years of GRACE data achieve a maximum degree of the expansion of 150–180 (Tapley et al. 2007; Förste et al. 2008a; Jäggi et al. 2009; Mayer-Gürr et al. 2010a).

The GOCE satellite (Drinkwater et al. 2003) was successfully launched on 17 March 2009 and started its operational phase in September 2009. Its mission objective, expressed as cumulated geoid accuracy, is 1–2 cm error at harmonic degree 200, which corresponds to a half-wavelength of about 100 km. To put this accuracy requirement into context, the estimated cumulated geoid accuracy of the combined model EGM2008 (Pavlis et al. 2008) is 7 cm at degree 200, whereas it is 20 cm at the maximum degree 180 for the satellite-only model ITG-Grace2010s (Mayer-Gürr et al. 2010b). GOCE is equipped with a gravity gradiometer as well as a GPS receiver to achieve this unprecedented performance. Satellite gravity gradiometry (SGG) data alone are not sufficient to accurately determine the low-degree coefficients of the gravity field due to the noise characteristics of the gradiometer. The GPS satellite-to-satellite tracking (SST) data are used to determine the precise orbit, thus geo-locating the gravity tensor observables, and the long-wavelength part of the gravity field. The models described in this paper are constructed with 71 days of data, i.e. just a little more than one full repeat cycle of 61 days. The choice of 71 days was driven by the fact that they composed the maximum amount of quality-checked GOCE data available at the time the scenario for this first gravity field solution was defined within the HPF project. With these first models we do not target the mission objectives of 1–2 cm geoid height and 1 mGal gravity anomaly accuracy, but rather aim at exploiting these novel data to the best possible extent and at evaluating the added value of GOCE data.

All pre-GOCE models have in common that the quality of the data reduction depends on the accuracy with which the satellite dynamics were reconstructed. This is not the case for gradiometer observations, which are direct measurements of the second derivatives of the gravitational potential. Consequently, a linearization of the observation equations and thus an iterative adjustment procedure is not necessary. In principle, for the geo-location of the gravity gradients by means of GPS an accuracy of 5–10 m would be sufficient. A scientific challenge arises due to the coloured noise of the gradiometer. Its measurement is very precise only in the measurement bandwidth (MBW) between 5 and 100 mHz (i.e. 200 to 10 s, respectively), and some sort of filtering is therefore an essential new component of the data processing procedure. Further, the gravity field models must be developed to high degree and order, and this task is rather demanding in terms of computer resources. Because of the complexity and sizeable effort needed for the gradiometer data reduction in particular, and due to the fact that gravity gradients are a completely new measurement type, it was decided to implement three different gravity field modelling approaches in the GOCE High-level Processing Facility (HPF; Rummel et al. 2004): direct (DIR), time-wise (TIM) and space-wise (SPW). In this way, HPF wanted to obtain the best possible model while simultaneously comparing the pros and cons of the three approaches, which are based on different and complementary processing philosophies. The direct approach (DIR) and the time-wise approach (TIM) assemble and solve large normal equation

systems to estimate the harmonic coefficients as parameters. While DIR starts with an a priori gravity field model and adds GOCE information to improve it, the rationale of TIM is to compute a GOCE-only model in a rigorous sense, which is solely based on GOCE data. In contrast, SPW works predominantly in the space domain, applying least squares collocation and exploiting spatial correlations of the gravity field.

The purpose of this paper is to describe the GOCE data reduction schemes and the subsequent gravity field computation using only the first cycle of data. Section 2 provides a description of the functional and stochastic models, and Sect. 3 gives a brief overview of the data sets used. The specificities of the three approaches are presented in Sect. 4. In Sect. 5 the results of the three GOCE models are assessed and compared, and the complementary properties of the solutions are discussed. In Sect. 6, the GOCE models are validated against existing gravity field information, and the added value of GOCE is evaluated. Conclusions and an outlook are provided in Sect. 7.

2 Functional and stochastic model

The functional model chosen to represent the anomalous potential $V(r, \vartheta, \lambda)$ in spherical coordinates (with radius r, co-latitude ϑ, longitude λ) is a series of spherical harmonics truncated at maximum degree N:

$$V(r, \vartheta, \lambda) = \frac{GM}{a} \sum_{n=2}^{N} \sum_{m=-n}^{n} A_{nm} \left(\frac{a}{r}\right)^{n+1} Y_{nm}(\vartheta, \lambda) \qquad (1)$$

where G is gravitational constant, M mass of the Earth, a equatorial radius of the Earth ellipsoid, and Y_{nm} surface spherical harmonics of degree n and order m:

$$Y_{nm}(\vartheta, \lambda) = \bar{P}_{n|m|}(\vartheta, \lambda) \begin{cases} \cos m\lambda & m \geq 0 \\ \sin |m|\lambda & m < 0 \end{cases} \qquad (2)$$

$\bar{P}_{n|m|}(\vartheta, \lambda)$ are the fully normalized associated Legendre functions, and $A_{nm} = \{C_{nm}, S_{n|m|}\}$ are the spherical harmonic coefficients to be determined, with C_{nm} for $m \geq 0$, and $S_{n|m|}$ for $m < 0$.

Gradiometric observations V_{ij} are point-wise measurements of the second-order derivatives of the gravitational potential

$$V_{ij} = \frac{\partial^2 V}{\partial x_i \partial x_j} \qquad (3)$$

which are obtained after separation from angular and centrifugal acceleration terms (Bouman et al. 2011). The measurements are performed in the gradiometer reference frame (GRF) defined by x_i, with $i, j = 1, 2, 3$, denoting the X, Y and Z direction of the GRF. The definition of the involved co-ordinate systems and their interrelation can be found in EGG-C (2010a).

In addition, the SST equations, together with the vector of non-gravitational accelerations, can be used in very much the same way as for the CHAMP mission (e.g. Reigber et al. 2002; Mayer-Gürr et al. 2005; Jäggi et al. 2010). This means that either an orbital analysis is performed, as in the direct method, or the so-called energy integral method (Jekeli 1999; Visser et al. 2003) is applied, as in the time-wise and space-wise approaches. One has to remark that the use of the energy integral method reduces the available orbit information by a factor of $\sqrt{3}$ when combining it into a unique scalar equation (Ilk and Löcher 2005).

Moreover it has to be recalled that, since the GOCE target is the knowledge of the static gravitational potential, corrections have to be applied to the observation equations in order to remove time varying effects like luni-solar attraction, tides and non-tidal effects. It should be emphasized that the final gravity field solution might be affected by errors of background model. This is especially true for model errors of the solar tide, which cannot be distinguished from static gravity field signals due to the sun-synchronous GOCE orbit.

The gradiometer measurements are performed most accurately and correspond to a flat (i.e. nearly white) power spectral density (PSD) only within the MBW of 5–100 mHz. Below and above the MBW, the frequency-dependent errors increase approximately with $1/f$ and f^2, respectively, where f denotes the linear frequency. The $1/f$ gradiometer error below the measurement bandwidth results in large long-wavelength errors in the measurement time series. As a consequence of this coloured noise behaviour, within the whole spectral range the gradiometer data are highly auto-correlated in their six tensor components (Schuh et al. 2006).

Figures 1 and 2 show the estimated gradiometer noise of the gravity gradient component V_{ZZ} as a time series, and in

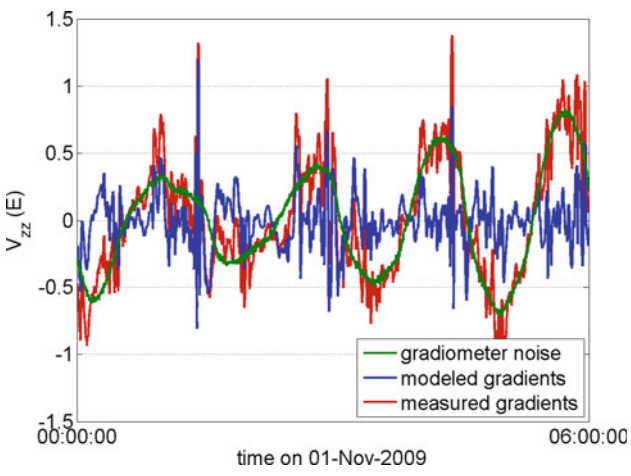

Fig. 1 Time series of the gradiometer noise of the V_{ZZ} component in comparison with the signal derived from EIGEN-5C. All curves have been reduced by GRS80 normal field and mean value

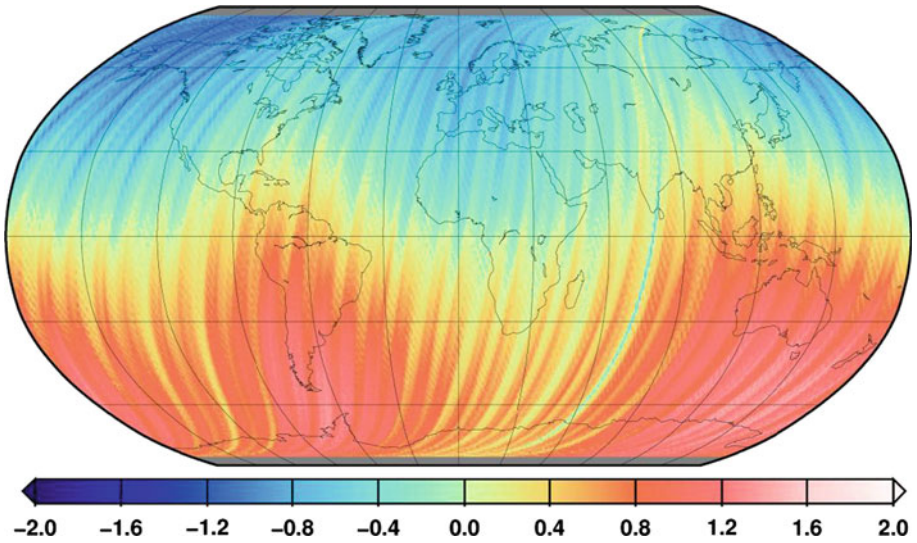

Fig. 2 Spatial distribution of the gradiometer noise (Eötvös) for the descending tracks of the V_{ZZ} gravity gradients (defined in the GRF)

the spatial domain by projecting them on a global grid, based on the 71-day data period. The noise time series represent residuals of a gravity field adjustment and have been obtained as the difference between the measured gravity gradients given in the GRF, and the adjusted gravity gradients in the GRF based on the estimated gravity field model. The noise is dominated by a long-wavelength term, which corresponds to a frequency of 1 cycle per revolution (cpr). A comparison of the estimated mean-removed noise (green curve in Fig. 1) with a signal modelled from a reference gravity field model (gravity gradients are computed from the EIGEN-5C model (Förste et al. 2008b) and reduced by the GRS80 normal field; blue curve in Fig. 1) shows that both are on the same order of magnitude, which clearly demonstrates the need for an adequate stochastic modelling of the measurement noise. In addition Fig. 1 shows the measured gradients (red curve), again reduced by GRS80 and the mean value. Figure 2 shows the spatial distribution of the gradiometer noise exemplarily for the descending tracks of the V_{ZZ} gravity gradients. Again the dominant long-wavelength component is evident.

The PSDs in Fig. 3 reveal further important aspects of the noise characteristics:

- very high power (indicating insensitivity of the gradiometer) and sharp peaks in the low-frequency domain (at multiples of 1 cpr);
- the components V_{XX}, V_{YY}, V_{ZZ}, and V_{XZ} have similar accuracies within the MBW, whereas the noise levels of V_{XY} and V_{YZ} are at two orders of magnitude higher (hence the latter two components are not used for gravity field determination); unfortunately, within the MBW the V_{ZZ} component (blue curve) performs worse than the other two main diagonal components V_{XX} and V_{YY} (red and green curves) by a factor of about 2. The reason for this degradation is still under investigation.

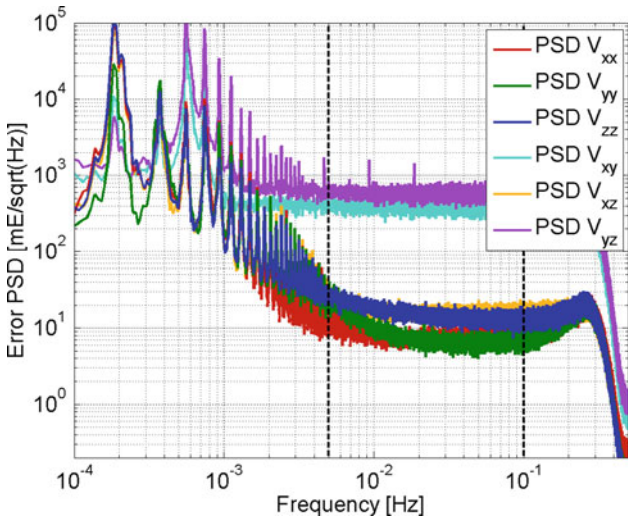

Fig. 3 PSD of the gradiometer noise for all six gravity gradient tensor components

For the gravity field solution to be consistently estimated by a least squares or collocation approach, these stochastic data characteristics must be properly taken into account either by means of the full data variance/covariance matrix or by means of an equivalent full data decorrelation/homogenization, which is accomplished very efficiently by digital filtering. In fact, one of the key differences among the three gravity field approaches is their strategy of taking the stochastic behaviour of the gradiometer into account:

- DIR: Autoregressive moving average (ARMA) filtering within the MBW only (cf. Sect. 4.1; Marty et al. 2005).
- TIM: ARMA filtering of the entire spectra, corresponding to a full data decorrelation (cf. Sect. 4.2; Schuh 1996, 2002; Siemes 2008; Schuh et al. 2010; Pail et al. 2010).
- SPW: Collocation approach after applying orbital Wiener filtering to the noisy gravity gradients and consistent

modelling of the signal and noise covariance functions (cf. Sect. 4.3; Tscherning 2001; Migliaccio et al. 2004; Reguzzoni and Tselfes 2009).

3 Data sets

The first GOCE gravity field models derived in the frame of HPF are based on the data period from 01-11-2009 to 11-01-2010, thus covering slightly more than one full GOCE orbit repeat cycle of 61 days. The following key products have been used (product identifiers according to EGG-C (2010a):

- Precise Science Orbits: SST_PSO_2I, including the sub-products:
  - SST_PKI_2I: kinematic orbits
  - SST_PCV_2I: variance-covariance information of orbit positions
  - SST_PRD_2I: reduced-dynamic orbits
  - SST_PRM_2I: quaternions for transformation from Earth-fixed to inertial reference frame.
- Gravity Gradients in the GRF: EGG_NOM_2
- Common (and differential) mode accelerations: EGG_CCD_2C
- Attitude Quaternions: EGG_IAQ_2C (corresponds to columns 56 to 59 of EGG_NOM_2; cf. EGG-C 2010a).

The gravity gradient product EGG_NOM_2 and precise science orbits SST_PSO_2I have been computed by HPF partners, cf. (Bouman et al. 2011; Bock et al. 2011).

Since the main objective is to derive a static gravity field, time-variable signals have to be reduced a priori from the SST and SGG measurement time series. Correspondingly, models for temporal gravity field reduction, such as ephemerides of Sun and Moon (AUX_EPH), ocean tide models (ANC_TIDE, ANC_TID_2I), correction coefficients for non-tidal temporal variation signals (SST_AUX_2I), and for Earth rotation (AUX_IERS) have been applied.

It shall be emphasized that not all of these different data types and sub-products are used by the three approaches (cf. Sect. 4). GOCE standards as defined in the GOCE Standards document (EGG-C 2010b) were consistently applied during the whole processing.

The following reference gravity field models, which are either exploited as a priori information, or for assessment and validation of the gravity field results, are used:

- EIGEN-5S and EIGEN-5C (Förste et al. 2008b)
- EGM2008 (Pavlis et al. 2008)
- ITG-Grace2010s (Mayer-Gürr et al. 2010b)
- AIUB-CHAMP03S.

Additionally, the very recently published model EIGEN-51C (Bruinsma et al. 2010) has been used only by the DIR method for internal validation purposes (cf. Sect. 4.1). Further, the SPW approach uses the GOCE Quick-look gravity field model (Mayrhofer et al. 2010; cf. also Sect. 4.2) as priori information (cf. Sect. 4.3).

4 Gravity field modelling: three HPF approaches

4.1 Direct approach (DIR)

4.1.1 Direct approach philosophy

Gravity field modelling using the direct approach is based on the least-squares solution of the inverse problem. The partial derivatives for all parameters to be adjusted, i.e. the spherical harmonic coefficients, are computed and normal equations are generated by processing data in 24-h batches, i.e. daily arcs. The daily normal equations are then stacked for the entire period and this resulting normal matrix is inverted using Cholesky decomposition. The computation of normal equations makes this approach very demanding in terms of CPU time and speed, number of CPU's, memory and disk usage. This is due to the large number of unknowns (and thus the size of the normal matrix), about 40000 at degree 200, paired to a large number of observations.

4.1.2 Data reduction procedure

SST data processing Data reduction is done in two separate steps because of the different nature of the SST and SGG processing techniques. The GPS SST observations are in fact not directly used, but substituted by the orbit positions of the reduced-dynamic precise science orbit (SST_PRD). The initial data weights were 15 mm for X, Y and Z positions. The SST data were processed in daily arcs in a classical orbit perturbation scheme, namely dynamic orbit computation in an iterative least-squares adjustment followed by normal equation computation. The background gravity field model was EIGEN-5C (Förste et al. 2008b; Flechtner et al. 2010) to degree/order 200, whereas the non-gravitational forces were provided by the common mode accelerometer observations. For a complete description of the force modeling, we refer to the GOCE standards (EGG-C 2010b). For each of the 71 daily arcs processed, of which 8 were rejected for various reasons, the parameterization as listed in Table 1 was applied. The small signal in the X direction thanks to the drag compensation and the frequent estimation of biases in the Y and Z directions enables the use of accelerometer data that are outside the MBW. The averaged RMS of the orbit fit to the SST_PRD positions is 1.5 mm.

Table 1 Estimated arc-dependent and global parameters of the GOCE SST processing

Arc-dependent parameters	Global parameters
Initial state-vector	Spherical harmonic coefficients for degrees 2 through 120
1-cpr accelerations per 3h in the radial, transversal and normal flight directions Accelerometer biases: X-bias per day, Y-bias per 3h, Z-bias per 3h	

SGG data processing The SST_PRD positions were used to geo-locate the gravity gradients, defined in the GRF, which have already been corrected in the pre-processing step (Bouman et al. 2011). Separate normal equations for each SGG component were then computed directly from the filtered observation equations in a single step. The initial data weights were 6, 6 and 9 mE for the V_{XX}, V_{YY}, V_{ZZ} gravity gradients, respectively. The background gravity field model was EIGEN-5C to degree/order 360, and partial derivatives for harmonic coefficients for degrees 2–240 were computed. A total of 71 daily batches were processed. Figures 1, 2, 3 clearly demonstrate the necessity of filtering the SGG observations, a procedure which aims at retaining the signal only within the MBW. The DIR approach opts to suppress the signal outside the MBW because in this way the result is largely independent of the variability in the coloured noise. Therefore, the (linearized) inverse techniques that allow the estimation of the spherical harmonic coefficients of the underlying gravity field model from observations cannot be applied as such. The measurements minus modelled quantities, the gravity gradient residuals, are all filtered together with the observation equations that relate these quantities to the unknown model parameters. Thus, a system of equations of the following form is filtered, where y_i are the observations, A is the design matrix, and which is written for P parameters x_j and a series of increasing epochs i:

$$y_i = \sum_{j=1}^{P} A_{ij}\, x_j \tag{4}$$

An ARMA filter was implemented. Its general expression is

$$\bar{y}_n = \sum_{k=0}^{N_a} \alpha_k\, y_{n-k} \; - \sum_{k=1}^{N_b} \beta_k\, \bar{y}_{n-k} \tag{5}$$

in which the bar stands for a filtered quantity and α and β are the filter coefficients. The transmittance of the filter is assumed to have the following form (i.e. decomposed as a product of second-order cells):

$$H(z) = \prod_{k=1}^{[N+1]/2} \frac{a_o^k + a_1^k z^{-1} + a_2^k z^{-2}}{b_o^k + b_1^k z^{-1} + b_2^k z^{-2}} \tag{6}$$

The derivation of the α and β coefficients from the a's and b's can be done using standard analytical and numerical procedures (e.g. Oppenheim and Schafer 1999).

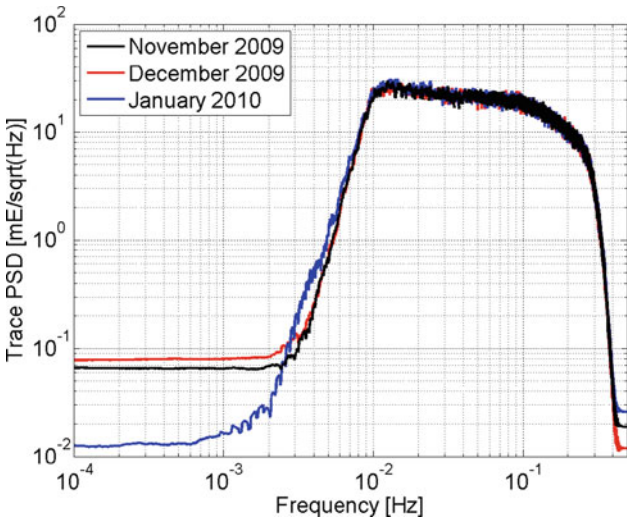

Fig. 4 Amplitude spectra of the trace for 2 days in November 2009 (*black*), December 2009 (*red*), and January 2010 (*blue*), respectively

The PSD of the trace after filtering, applying an 8th order band-pass filter with a pass band of 10–125 mHz (corresponding to [100-8] seconds), is shown in Fig. 4. The three curves represent the smoothed PSDs for two days in November 2009, December 2009 and January 2010, respectively. This filter attenuates the low frequencies to less than 0.1 mE in the stop band, whereas the signal in the pass band remains unchanged. The pass band represents along-track spatial scales of approximately 800 through 64 km assuming a speed of 8 km/s (8×100 through 8×8), which resolution roughly translates to spherical harmonic degrees 25 through 312 (degrees 20,000 km/800 km through 20,000 km/64 km).

Combining SST and SGG normal equations and solving The SST and SGG normal matrices are summed, after determining via trial and error the optimum relative weights, in order to cover both low and high degrees of the spectrum. The effect of the weighting was evaluated by means of the a posteriori variance of the solution, plotting residual maps and GOCE orbit computation results. Based on the above metric, the optimum combination of SST and SGG normal matrices was obtained by down-weighting the V_{YY} normal equation by 0.5, and the SST matrix by 0.05.

The combined SST+SGG normal matrix is solved by means of Cholesky decomposition. The regularization of the gravity field solution, necessary due to the polar gaps,

is done using the spherical cap regularization (Metzler and Pail 2005). The geopotential function is given as an analytical continuous function over the polar regions only, i.e. in the polar caps. The regularized normal system has the form described by Eq. (27) in the above-referenced paper, and the stabilizing function on the right-hand side of the regularized normal system was chosen as a spherical harmonic expansion of the potential based on the model EIGEN-51C (Bruinsma et al. 2010). This combined model complete to degree/order 360 is based on 6 years of CHAMP and GRACE data and the DNSC08 global gravity anomaly data set (Andersen and Knudsen 2009). Radii of the polar gaps were taken as 6.5°, and all necessary integrations over co-latitude were prepared analytically in the direction from south to north.

GOCE gravity field solutions were evaluated by comparing with EIGEN-51C and ITG-Grace2010s, as well as by means of orbit and GPS leveling tests.

In summary, the processing procedure consists of the following four steps, which were (partly) re-iterated for each model version produced:

1a. Compute SST normal equations for cycle 1.
1b. Compute SGG normal equations for cycle 1.
2. Sum all SGG and SST normal matrices.
3. Solve using regularization.
4. Evaluate solution accuracy.

4.1.3 Filter selection

The effect on the gravity field recovery due to filtering was determined by processing the entire SGG data set using filters with varying high-pass cut-off frequencies from 4 through 10 mHz (the low-pass cut-off was always 125 mHz), i.e. steps 1b to 4. For the different filtered SGG data sets we computed SGG-only solutions for the V_{ZZ}-component, which were stabilized by the mentioned spherical cap regularization. These resulting solutions were compared with our reference model EIGEN-51C, in particular to evaluate the low degrees, which are much less accurate in a GOCE-only solution. It is worth mentioning that EIGEN-51C was selected as the reference instead of EIGEN-5C after the GOCE SGG data revealed the much better performance of the former model, especially over Antarctica, South America, Africa, the Himalayas and New Guinea (see Sect. 6). The degree median spectra of the mentioned V_{ZZ}-only solutions compared with EIGEN-51C are shown in Fig. 5. Furthermore, the degree median difference between EIGEN-51C and ITG-Grace10s is given as an approximate guideline for the accuracy of recent GRACE models. Since the GOCE solution is inferred from 2 months of data the degree median differences between a two-month GRACE-only solution (from November and December 2007) and EIGEN-51C is given additionally as comparison. Figure 5 demonstrates the effect of the different filters, namely an abrupt decrease of the curves of the solutions below degree 20, 30 and 40, respectively (below these abrupt decreases the GOCE solutions are more or less identical with the a-priori field applied in the spherical cap regularization). The curves move to the right and the differences with EIGEN-51C as well as with the two-months' GRACE-only solution within the measurement bands (i.e. beyond the abrupt decreases) become smaller for decreasing cut-off periods. The GRACE-inferred model EIGEN-51C is almost two orders of magnitude more accurate for the low degrees. Therefore, we selected the 10–125 mHz band-pass filter, which produced the smallest differences in this spectral range.

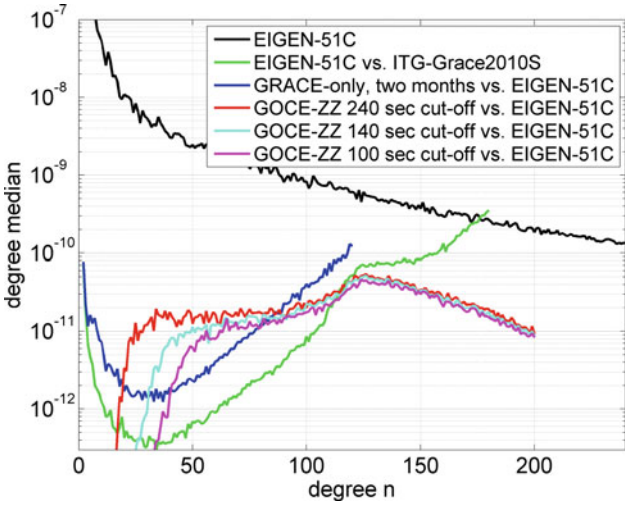

Fig. 5 Degree-variance spectra of GOCE SGG-ZZ only solutions (direct approach) obtained with different filters compared with EIGEN-51C: (1) EIGEN-51C; (2) EIGEN-51C versus ITG-Grace10s; (3) a GRACE-only 2-months solution versus EIGEN-51C; (4, 5, 6) GOCE SGG-ZZ-only solutions versus EIGEN-51C for 240, 140 and 100 s high-pass cut-off periods

4.1.4 The constrained gravity field model

The summed SST and SGG normal equations were solved to degree/order 240 after applying spherical cap regularization to the same maximum degree; without regularization, the solutions are inaccurate due to extreme correlations between coefficients. Simply put, this regularization forces the solution to be equal to the reference model, i.e. EIGEN-51C, in the unobserved polar caps of 6.5° spherical radius. This is clearly visible in Fig. 6 over Antarctica.

To investigate the effect of the applied spherical cap regularization, a fully unconstrained solution of the combined SST+SGG normal matrix has been computed for comparison. Figure 7 displays the differences in the estimated spherical harmonic coefficients C_{nm} and S_{nm} between the unconstrained solution and the regularized and published

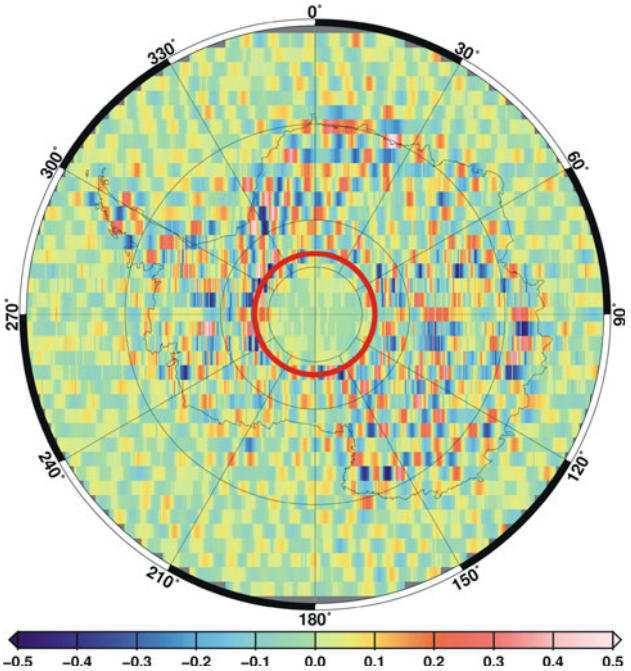

Fig. 6 Geoid height differences (m) over the south pole between the GOCE gravity field from DIR and the reference field EIGEN-51C, which has been used for the spherical cap regularization. The GOCE polar gap is indicated by a *red circle*

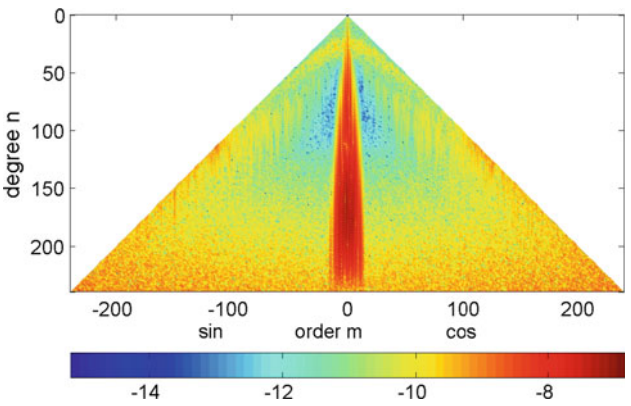

Fig. 7 Differences in the estimated spherical harmonic coefficients C_{nm} and S_{nm} due to regularization, displayed in $\log_{10}$ scale

DIR solution, which are due to the regularization, in logarithmic scale. As expected, the largest differences are in the zonal and near-zonal coefficients, as well as the sectorials. However, all other coefficients are different from the unconstrained solution, too, due to correlations, but these differences are 2–3 orders of magnitude smaller. This type of regularization should not be necessary when directly combining GOCE with GRACE data thanks to the latter satellites' polar orbit.

4.2 Time-wise approach (TIM)

4.2.1 Software architecture

The time-wise approach considers the gravity gradient and orbit observations as time-series measured along the satellite orbit. This is especially beneficial considering the highly correlated gravity gradient observations described in Sect. 2. Gravity field determination methods in time and frequency domain are applied to these observation time series.

The main processing philosophy is to derive a pure GOCE-only model, i.e. no gravity field prior information shall enter the solution, not even as a reference model. Correspondingly, the gravity field coefficients are estimated from scratch, and several dedicated processing strategies have been developed and applied to guarantee independence of a priori gravity field information. The key idea of this pure GOCE-only solution is to evaluate what GOCE can do on its own. It is useful to have a GOCE solution which is completely independent of GRACE and terrestrial data, because in this case a direct comparison with this complementary gravity field information can be made, and potential insufficiencies can be detected.

The software system for time-wise gravity field modelling is composed of two main components: the Quick-Look Gravity Field Analysis (QL-GFA; frequency domain), and the Core Solver (CS; time domain). The main purpose of the stand-alone gravity field solver QL-GFA, which is based on a semi-analytical method, is to derive a fast diagnosis of the GOCE system performance and of the Level 1b and Level 2 input data in parallel to the mission with short latencies as part of ESA's calibration/validation activities. QL-GFA is an additional tool exclusively operated by the time-wise processing system. A detailed description of the architecture design and functionality of the QL-GFA processor can be found in Pail et al. (2007b), and first operational results are provided in Mayrhofer et al. (2010).

The CS delivers a rigorous solution of the very large normal equation systems applying parallel processing strategies. The Core Solver is composed of the Final Solver (FS), taking the full normal equation matrix into account, and the Tuning Machine (TM), being based on the method of preconditioned conjugate gradients (pcgma; Schuh 1996) and working with sparse matrices. The main task of the TM is to verify and tune the involved software components of the FS. The main modules of the CS are

- SST processor: gravity field modelling from orbits applying the energy integral approach in an inertial reference frame (Badura 2006).
- Tuning Maching: consists of the full-fledged gravity solver *pcgma* (Boxhammer and Schuh 2006), which is used to derive optimum regularization and weighting parameters, and the *Data analysis tool*, which performs

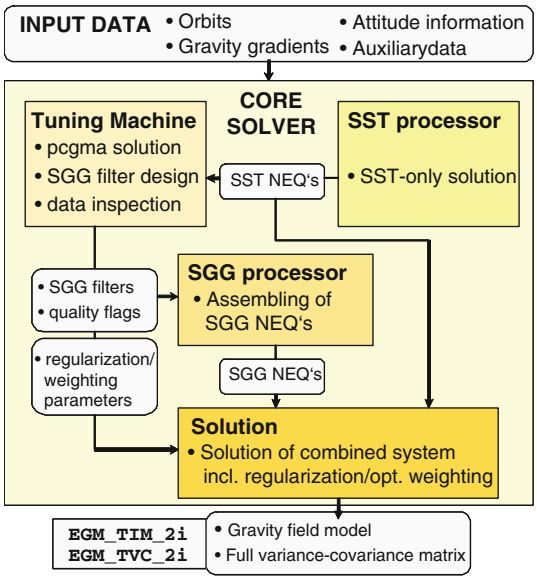

Fig. 8 Software architecture and product flow of the time-wise gravity field processing

outlier detection and delivers the SGG filter models which will be used in the FS to introduce the stochastic observation models.

- SGG processor: assembling of the full SGG normal equations applying parallel processing on a Linux-PC-Cluster (Pail and Plank 2002).
- Solver: rigorous combined SST and SGG solution by means of superposition of the normal equations, applying an optimum weighting of the individual data types based on variance component estimation (Koch and Kusche 2002; Brockmann et al. 2010). The solution is processed applying a parallelized Cholesky reduction.

Figure 8 shows the software architecture and product flow of the CS. A detailed description of the processing scheme can be found in Pail et al. (2007a).

4.2.2 Gravity field processing and results

SST processing Kinematic orbits (SST_PKI), which are purely geometrical orbit solutions based on the GPS observations without including any gravitational and non-gravitational force models, are used for the TIM gravity field model, although detailed analyses have shown that a substantially better performance could have been achieved when using the reduced-dynamic orbits (SST_PRD). However, since the latter orbit type is heavily biased towards the GRACE prior model, its use would have violated our main goal to derive a GOCE-only model.

The energy integral method was applied to assemble and solve the SST normal equation system resolved up to degree/order 100. The variance information of the kinematic orbit positions (SST_PCV) has been used as stochastic model, because the orbit errors turned out to be latitude-dependent, which is related to the geometry of the GPS configuration. Thus, by including this error information, the SST normal equation system reflects the true error behaviour, which is an important issue also for an optimum weighting when combined with the SGG normal equations later on.

Tuning machine In addition to the outlier detection activities performed in the frame of the pre-processing in SPF3000 (Bouman et al. 2011), applied to the full gravity field signal, here we apply outlier detection also to the residuals of the gravity field adjustment in the course of the iterative TM processing. The main advantage is that the residuals have much smaller amplitudes, and thus outliers become more distinct.

Another key element of the time-wise processing philosophy is the correct stochastic modelling of the gradiometer errors (cf. Fig. 3) over the whole spectral bandwidth. Digital filters are used to set-up the variance–covariance information of the gravity gradient observations (Schuh 1996, 2002, cf. also equations (4) to (6)). Since the full variance–covariance matrix of the several million observations is too large to be stored even on a supercomputer, the idea of describing their noise characteristics by an ARMA process was developed (Schuh 1996). The inverse process, which can be interpreted as a digital filter, is used to decorrelate the observations and the corresponding functional model. Technically, this is done by applying these digital filters to the full observation equation, i.e. both to the observations and the columns of the design matrix. Thus, the gradiometer error information is introduced as the metrics of the normal equation system. It should be emphasized that by this strategy the full spectral range of the gravity gradients enters the gravity field solution, but they are properly weighted according to their spectral behaviour.

The red curve in Fig. 9 shows the error PSD of the gradiometer component V_{ZZ} as it was estimated from the residuals of a previous gravity field adjustment. (It corresponds to the blue curve in Fig. 3.) Filter models of different complexity have been fit to this error PSD (Schuh et al. 2010). The most obvious features are the peaks at frequencies of multiples of 1 cpr (cf. also Fig. 3), mostly below the MBW. They can either be modeled peak by peak (green curve), or as some average (blue curve). Different filter models have been applied to compute gravity field models, and their performance has been assessed and cross-validated. The final validation of this multitude of different gravity field model results revealed that a less complex filter model (blue curve) is sufficient for all three gravity gradient components V_{XX}, V_{YY} and V_{ZZ}. As a decision criterion for this validation, it was evaluated whether there are significant changes in the resulting gravity field solutions and corresponding residuals when applying

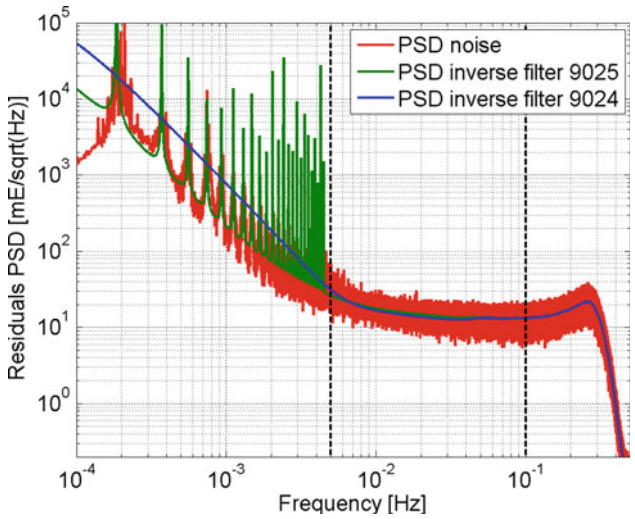

Fig. 9 Gradiometer noise and different SGG filter models of gravity gradient component V_{ZZ}

different filter models. Key advantages of this less complex filter model are that it has a relatively short filter order of 52 (and thus is computationally efficient) and a short warm-up time of only 2000 s, while the drawback of more complex filter models are warm-up times of one day or even longer until the correct filter performance is achieved. However, for future GOCE gravity field models, which are based on longer measurement periods than the present 71 days, it is foreseen to apply more complex filter models, which represent the true stochastic behaviour even better. A more detailed discussion on the refinement of the stochastic model for this GOCE solution is given by Schuh et al. (2010).

SGG assembling and combined solution After SST processing and diverse tuning steps, the full SGG normal equations complete to degree/order 224 have been assembled on a Linux-PC-Cluster (Pail et al. 2007a), using only the three main diagonal components V_{XX}, V_{YY} and V_{ZZ}, defined in the GRF. It could be shown that the fourth high-accuracy gravity gradient component V_{XZ} (cf. Fig. 3) can add only marginal contributions to the solution due to its sensitivity to attitude errors (Pail 2005). Finally, the combined solution was processed by addition of the SST and SGG normal equations, and applying regularization and optimum relative weighting based on variance component estimation (Koch and Kusche 2002). The relative weights of SST and SGG turned out to be 0.20 and 1.01, respectively.

Special emphasis has to be given to constraining the combined normal equation system. Two different approaches have been investigated. The spherical cap regularization approach (Metzler and Pail 2005), a regularization technique which is dedicated to the specific problem of the non-polar orbit configuration of the GOCE satellite and the resulting polar gaps, was applied. Since one of the main goals is to compute a GOCE-only solution, the choice of the stabilizing function in the polar areas is a critical issue. In order to fulfil this requirement, an independent SST-only solution complete to degree/order 50 was computed based on the kinematic orbit. Due to the lower cut-off degree, such a solution is only slightly affected by the polar gap problem. This solution was then used to compute the stabilizing function in the polar gap regions. The spectral leakage effect inherent in this low-degree SST-only solution was a priori estimated to be in the order of 2 m. Since the polar caps are filled again with GOCE information, this solution can be considered as a pure GOCE model in a rigorous sense.

As a second approach, Kaula regularization was applied, but only to selected groups of coefficients. The first group involves all zonal and near-zonal coefficients, which are affected by the polar gap, according to the rule of thumb given by Sneeuw and van Gelderen (1997). As the second group, Kaula regularization was also applied to coefficients with degrees larger than 170 in order to improve the signal-to-noise ratio in the very high degrees. It is important to emphasize that since we do not use any reference gravity field model for our solution, it is Kaula constrained towards a zero model, but not towards a reference gravity field. Figure 10 demonstrates the effect of constraining the solution. It shows degree medians of the deviations of the GOCE solutions from EIGEN-5C (Förste et al. 2008b). Evidently, compared with the unconstrained solution (red curve), the constrained Kaula solution (blue curve) shows significantly lower energy in the very high degrees.

In order to show the impact of these constraints more lucidly, Fig. 11 illustrates the GOCE redundancy factors (Sneeuw 2000) of the constrained solution. It expresses the "GOCE-onlyness" of the solution, i.e. to which extent GOCE

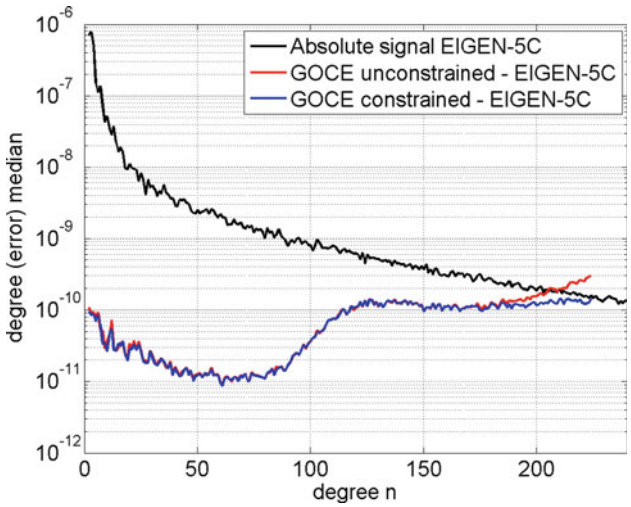

Fig. 10 Degree medians of constrained versus unconstrained TIM solution

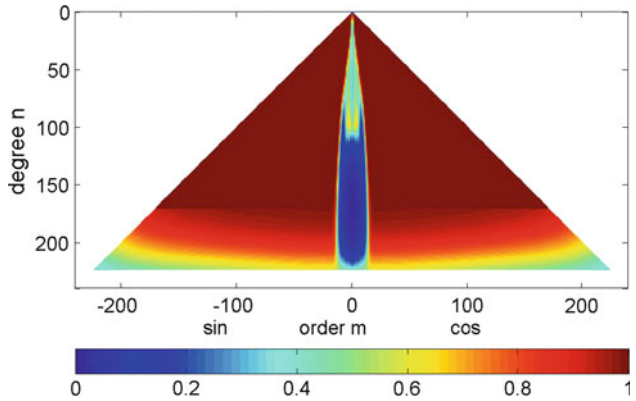

Fig. 11 Redundancy factors of constrained TIM solution. A value of '1' means that a certain coefficient is determined solely from GOCE information

information was used for the estimation of specific harmonic coefficients. Correspondingly, a value of '1' means that a certain coefficient is estimated only from GOCE information, while a lower value indicates that the constraint towards zero is acting. These constraints are visible for (near-)zonal coefficients, and are gradually increasing with growing degree, starting from degree/order 170. For the unconstrained solution (not shown) all values would be '1', because kinematic orbits have been used also here for the low degrees, and the polar caps have been filled with GOCE information.

Eventually, due to the improved signal-to-noise ratio in the higher degrees, the constrained solution has been selected as the official and final TIM gravity field model.

4.3 Space-wise approach (SPW)

4.3.1 Space-wise philosophy

The main idea behind the space-wise approach is to estimate the spherical harmonic coefficients of the geopotential model by exploiting the spatial correlation of the Earth gravity field. For this purpose a collocation solution (Moritz 1989; Tscherning 2001) has been devised, modelling the signal covariance as a function of spatial distance and not of time distance, as it is instead done for the noise covariance. In this way, data which are close in space but far in time can be filtered together, thus overcoming the problems related to the strong time correlation of the observation noise.

Although theoretically clean and desirable, a unique collocation solution is computationally not feasible due to the huge amount of data of the GOCE mission. The dimension of the system to be solved would be in fact equal to the number of processed data.

For this reason, the space-wise approach is implemented as a multi-step collocation procedure (Reguzzoni and Tselfes 2009), basically consisting of

- a Wiener filter (Papoulis 1984) along the orbit to reduce the highly time correlated noise of the gradiometer,
- a spherical grid interpolation at mean satellite altitude by applying collocation on local patches of data (Migliaccio et al. 2007),
- a harmonic analysis by numerical integration (Colombo 1981) to derive the geopotential coefficients.

The whole procedure is iterated till convergence (see Fig. 12) to recover the signal frequencies cancelled by the Wiener orbital filter and to correct the rotation from gradiometer to local orbital reference frame. Note that the gravity field model derived by SST data is used as prior model to reduce the spatial correlation of the signal, which is necessary when applying collocation gridding on local patches of data.

It can be shown that this iterative procedure, apart from the numerical approximations due the local gridding, is equivalent to a unique and direct collocation from original data to spherical harmonic coefficients (Reguzzoni and Tselfes 2009).

Since the resulting strategy is quite complicated, an exact error covariance propagation is not feasible. As a consequence, the error covariance matrix of the estimated coefficients is derived by using Monte Carlo techniques (Migliaccio et al. 2009).

4.3.2 Space-wise data pre-processing

Although it is not the goal of the space-wise approach, data pre-processing (outliers and data gaps detection and correction) is a crucial activity to obtain a good gravity field solution. Remaining in the spirit of the space-wise approach, outliers and data gaps in the input data are replaced with values estimated by collocation after removing a reference signal to make the residuals as stationary as possible.

Here it is important to stress that the replaced values are only used in the time-wise steps (e.g. the Wiener filter along the orbit) when it is useful to have a continuous flow of data. In the core of the space-wise approach, i.e. in the gridding procedure by collocation, the values interpolated in the data gaps or in correspondence to outliers are not used, because the gridding procedure does not require that the input data are regularly sampled in time. This is an advantage of the space-wise philosophy.

4.3.3 Space-wise SST model

After pre-processing, the first step in the space-wise approach is the recovery of the low-frequency part of the gravity field

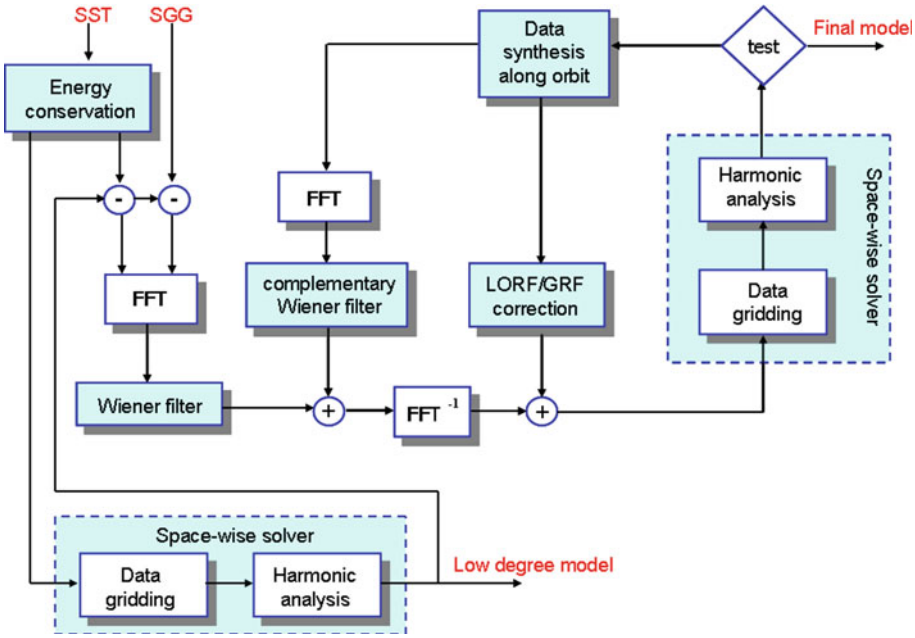

Fig. 12 The space-wise iterative scheme

from satellite tracking data; later on, this information will be used to reduce the long-period signal when dealing with gravity gradients.

Since the gravitational potential has been computed from kinematic orbits (SST_PKI), this implies the need of estimating satellite velocities from satellite positions. This is done by a least-squares polynomial interpolation over a moving window, also weighting the involved observations according to the position error estimates (SST_PCV); see Migliaccio et al. (2010b) for details.

The determination of the potential V along the orbit is done by the energy-conservation approach, also taking into account the effects of non-gravitational forces (atmospheric drag, solar pressure, etc.) and tides. The former are computed by exploiting the common mode accelerations of the gradiometer, after estimating and removing biases in the accelerometer data. The latter are modelled by using external information such as Sun and Moon ephemerides, ocean tidal models, etc. Error covariances for the potential are estimated by propagating the position errors first through the velocity interpolation procedure and then through the linearized energy conservation approach.

Note that, although the principle is the same, in the space-wise approach the energy conservation approach is used to obtain an explicit estimate of the gravitational potential, while in the time-wise approach it is used to directly estimate the SST spherical harmonic coefficients via least-squares adjustment.

In Fig. 13, the empirical and the estimated error power spectra are compared. The former is computed from the differences between the estimated potential along the orbit and the one synthesized from EGM2008, and the latter is

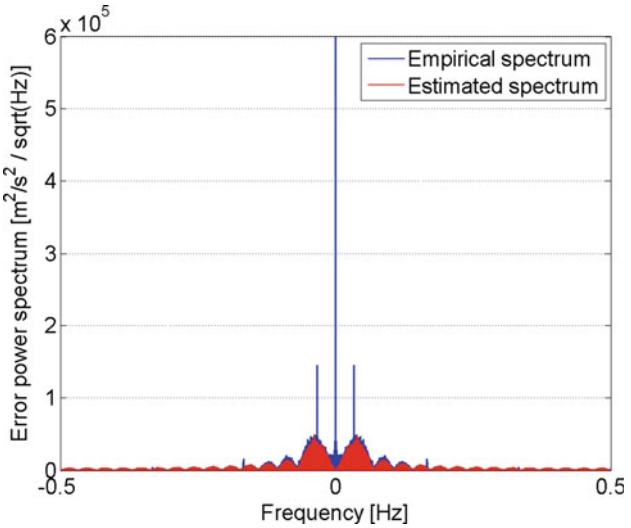

Fig. 13 Empirical (*blue*) and estimated (*red*) error power spectrum of the potential along the orbit

computed from the estimated error covariances with the additional assumption of stationarity in time. Two main differences can be noticed. First, there are spikes in the empirical spectrum indicating that some periodical behaviours are still present in the estimated "static" potential, probably because they are not completely removed when modelling tidal effects in the energy conservation approach; the frequency of the main spike corresponds to half orbital period. Second, the estimated error spectrum at very low frequencies is much lower than the empirical one; this discrepancy may be attributed to the use of unfiltered common mode accelerations in the computation of the non-gravitational force effects. In any

case, the estimated potential is modified in such a way that these differences are removed from the empirical error spectrum, thus introducing EGM2008 as prior information. This is the reason why the SST low spherical harmonic coefficients, approximately below degree 30, have much higher accuracy than expected from a GOCE-only solution based on kinematic orbits. Note that this data modification will not be applied in future releases of the space-wise gravity field model. Instead, it will be replaced with an improved modelling of the error covariance structure of the estimated potential.

The next step is the gridding at mean satellite altitude. When applying gridding in the space-wise approach, observables generated from a prior model are removed from the data and then added back to the solution (remove-restore procedure). Here, the idea is to remove from the estimated potential the one computed from a Quick-look model (Mayrhofer et al. 2010), which is a prior information ingested by the space-wise approach, but still related to GOCE data. However, the Quick-look model delivered by HPF for the considered time period is not entirely a GOCE-only model, because it makes use of reduced-dynamic orbits; for this reason, it has been degraded at low degrees. Despite this degradation, the Quick-look regularization in polar areas (spherical cap regularization using EIGEN-5C) has been inherited by the SST space-wise solution.

The degree variances σ_n^2 of the residual signal after removing the degraded Quick-look model are used as input in the collocation procedure. In particular, they are used to model the residual signal covariance function as

$$C_y(r, r', \psi) = \left(\frac{GM}{a}\right)^2 \sum_n \sigma_n^2 \left(\frac{a^2}{rr'}\right)^{n+1} P_n(\cos\psi) \quad (7)$$

where r and r' are the radii of the two considered points, while ψ is their spherical distance. $P_n(\cos\psi)$ are the Legendre polynomials of degree n.

The corresponding signal covariance matrix C_{yy} is derived from Eq. (7), while the noise covariance matrix C_{vv} comes from the estimated error of the computed potential along the orbit. Since this is not stationary in time, the noise covariance matrix does not have a Toeplitz structure.

The estimated grid values at mean satellite altitude with a grid size of $0.5° \times 0.5°$ are then derived by applying the usual collocation formula to local overlapping patches of data with a size of $20° \times 20°$:

$$\underline{\hat{y}}_{\text{grid}} = C_{y_{\text{grid}},y} \left(C_{yy} + C_{vv}\right)^{-1} \underline{y}_0 \quad (8)$$

$\underline{y}_0$ where is the vector of the "observed" gravitational potential, $\underline{\hat{y}}_{\text{grid}}$ is the estimated vector, and $C_{y_{\text{grid}},y}$ the potential cross-covariance matrix between points on the grid and along the orbit.

After the gridding, harmonic analysis by numerical integration has been implemented to estimate the spherical harmonic coefficients of the SST-only model:

$$\hat{c}_{nm} = \frac{\Delta^2}{4\pi a_n} \sum_i \sum_j \hat{y}(\vartheta_i, \lambda_j) Y(\vartheta_i, \lambda_j) \sin(\vartheta_i) \quad (9)$$

where $a_n = \frac{GM}{a}\left(\frac{a}{r}\right)^{n+1}$, and Δ is the angular grid side.

This simple version of the quadrature formula is used because its discretization errors are well below the noise level and it is more robust against aliasing than, for example a harmonic analysis by least-squares adjustment (Rummel et al. 1993). Moreover, a further weighting of the grid nodes is not necessary since the optimal filtering according to the Wiener Kolmogorov principle is already implemented in the previous gridding step.

4.3.4 Space-wise SST + SGG model

The final space-wise solution is computed according to the iterative scheme displayed in Fig. 12.

As already pointed out in the description of the other two gravity field determination strategies, a key issue in the SGG data processing is the filtering procedure. In the space-wise approach this is done at two different levels. First a Wiener filter along the orbit is applied, because the gradiometer noise is time-correlated, and therefore a time-wise filtering is the most natural choice. The application of this Wiener filter in the frequency domain requires the estimation of the signal and noise power spectra of the input data, which is done by making the usual hypothesis of time stationarity. For this reason the implemented Wiener filter is not optimal, because the input signal is not stationary due to the orbit wrapping. In other words, pairs of points at the same time distance do not have the same spatial distance, and since ultimately the gravitational signal is spatially correlated, the hypothesis of stationarity can be accepted at most up to half an orbit (Albertella et al. 2004).

The second level of filtering is implicitly implemented when reducing data to a spherical grid. This is done by collocation, disregarding the data time sequence and averaging observations that are close in space and hence contain the same or similar "static" gravity signal. This particular filtering exploiting the spatial correlation of the data is definitely the main characteristic of the space-wise approach.

From the practical point of view, the "optimality" of the spherical harmonic coefficient estimation according to the Wiener–Kolmogorov principle inside the iterative scheme of Fig. 12 is obtained by modifying the gridding collocation operator G as follows (see Reguzzoni and Tselfes 2009):

$$G = C_{z_{\text{grid}},y} \left(C_{yy} + WC_{vv}\right)^{-1} \quad (10)$$

where z_{grid} is the functional to be estimated on the grid (the potential V or its second radial derivatives V_{rr}), while y and ν, respectively, are the signal and noise of the input observations, i.e. the potential estimated by the energy conservation approach and the four gravity gradients that are accurately measured by the on-board gradiometer. W denotes the Wiener filter operator in the time domain.

Actually, the procedure is not optimal mainly because the collocation is not applied to the whole data set but to local overlapping patches of data with a size of $6° \times 6°$.

Before presenting results, it is important to discuss how the space-wise approach addresses the two issues of regularization and polar gaps.

Concerning the first one, the collocation procedure, which is at the basis of the whole space-wise processing chain, is itself a regularization method, in the sense that the estimation is "forced" to zero, i.e. to the mean value of the underlying random field, when the error is much larger than the signal. This regularization can be typically seen at high degrees, avoiding that the error degree variances become larger than the signal degree variances. This is very similar to the effect of Kaula's regularization implemented in the time-wise approach, with the only difference that there is not a chosen starting degree (which is 170 in the time-wise solution), but the regularization is automatically weighted and applied all over the whole spherical harmonic spectrum according to the modeled signal and noise covariances.

Concerning the polar gaps, this problem is solved by extrapolating grid values in the polar areas using the available GOCE observations. In this way no external information is introduced to fill polar gaps. Moreover, since the gridding is performed by collocation, the extrapolated grid values, and consequently the zonal and near-zonal coefficients, are again regularized according to the same principle described above.

At this point, some intermediate results of the space-wise approach are presented, i.e. the quality of the filtered data along the orbit and of the estimated grids at mean satellite altitude. These intermediate products can for instance be used for geophysical applications, because their local content is larger than the averaged global information provided by the final spherical harmonic coefficients. The production of these intermediate results can be considered another peculiarity of the space-wise approach.

The error rms of the filtered data along the orbit is reported in Table 2, both as differences with respect to the corresponding EGM2008 signal and as estimated error by Monte Carlo techniques. Empirical differences and estimated errors are in good agreement.

Some statistics on the accuracy of the estimated grids are reported in Table 3. The gravitational potential and the four gravity gradients reported in Table 2 are jointly used as input in the gridding procedure, producing spherical grids at mean satellite altitude with a resolution of $0.5° \times 0.5°$.

Table 2 Statistics of the time filtered data (ξ = almost along-track, η = cross-track, r = radial)

	V (m^2/s^2)	$V_{\xi\xi}$ (mE)	$V_{\xi r}$ (mE)	$V_{\eta\eta}$ $V_{(mE)}$	V_{rr} (mE)
Empirical error rms (w.r.t. EGM2008)	0.091	2.4	4.4	4.6	6.0
Estimated error rms (Monte Carlo)	0.089	2.5	4.2	4.6	5.9

Table 3 Statistics of the gridded data for $|\varphi| < 83°$

	V (m^2/s^2)	V_{rr} (mE)
Empirical error rms (w.r.t. EGM2008)	0.020	2.64
Predicted error rms (Monte Carlo)	0.016	1.44

Both functionals estimated on the grid have an analytical expression that can be easily integrated to estimate the spherical harmonic coefficients. In particular, the gravitational potential is more suitable to describe the low degrees of the field, while its second radial derivative is preferable for higher degrees. The two solutions are then combined into a unique set of coefficients on the basis of the estimated error variances. From the resulting coefficients, observables are synthesized, and the iterative space-wise scheme is repeated till convergence, finally obtaining the official and delivered SPW gravity field model (Migliaccio et al. 2010a).

The full error covariance matrix of the estimated coefficients is derived by Monte Carlo simulation using only 400 samples for computational time reasons. Note that the signal covariance modelling (and consequently the collocation operator) is based on degree variances, while the estimation error is obtained by generating Monte Carlo samples according to the single coefficient variances.

4.4 Overview of the three gravity field processing methods

As a summary of the previous detailed description of the three gravity field processing methods DIR, TIM and SPW, Table 4 provides an overview of their key features, as they have been discussed in the previous Sects. 4.1 to 4.3 in detail. The first line in the Table 4 provides the official name of the three models, which are available at the ICGEM webpage (http://icgem.gfz-potsdam.de/ICGEM).

The maximum degree of resolution of the three models was not co-ordinated a priori, but was chosen individually by the three processing teams. This choice is driven by the signal-to-noise ratio, processing issues and the strategy of using additional prior information.

5 Gravity field results

In this section, we assess and compare the three independent gravity field solutions, whose generation has been described

Table 4 Key features of the 3 gravity field processing strategies

	DIR	TIM	SPW
Gravity field model	GO_CONS_GCF_2_DIR	GO_CONS_GCF_2_TIM	GO_CONS_GCF_2_SPW
Rationale	Improvements by GOCE relative to prior model	Pure GOCE-only model	Model from grids of GOCE data
Prior model	EIGEN-5C	No prior gravity field information	EGM2008 (in very low degrees + Quick-look model)
Method	Least squares using full normal equations SST: numerical integration using reduced-dynamic orbits	Least squares using full normal equations SST: energy integral based on kinematic orbits	Orbital Wiener filter + least squares collocation SST: energy integral based on kinematic orbits
SGG stochastic modeling	ARMA filtering within the MBW	ARMA filtering of entire spectrum (full decorrelation)	Covariance functions (time-correlated for the noise and space-correlated for the signal)
Resolution	240	224	210

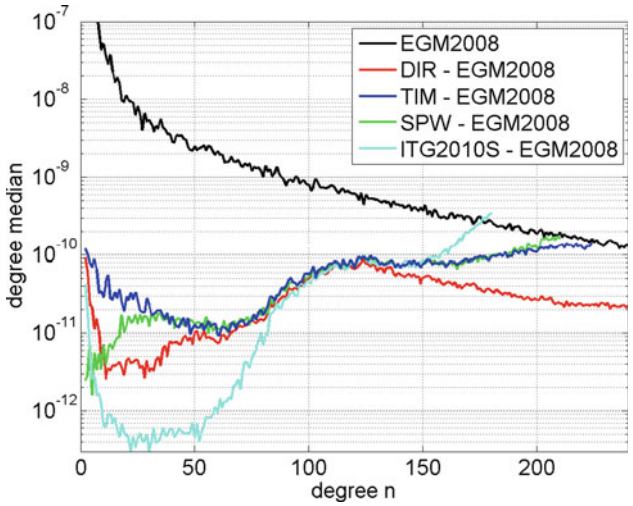

Fig. 14 Degree medians expressing differences of the three models DIR, TIM and SPW from EGM2008

in Sects. 4.1 to 4.3, on the basis of differences from existing gravity field models, their error estimates and derived quantities.

Figure 14 shows the differences of the three solutions from the reference gravity field model EGM2008 in terms of degree medians. It shows very nicely the characteristic features of the different approaches, which are resolved up to a different maximum degree: DIR ($N = 240$), TIM ($N = 224$), SPW ($N = 210$).

One of the most striking differences is their behaviour in the low degrees. The TIM gravity field model (blue curve) shows the largest deviations from EGM2008, because it is based solely on 2 months of kinematic GOCE orbits, with no external (GRACE) information (cf. Sect. 4.2). On the other hand, the DIR solution (red curve) uses reduced-dynamic orbits (cf. Sect. 4.1), and thus it is biased towards the background gravity field model EIGEN-5C, which is essentially GRACE information in this spectral region. An intermediate position in this context is taken by the SPW model (green curve), because EGM2008 was introduced as prior information for the lowest 20–30 degrees (cf. Sect. 4.3).

In the medium frequency range (degrees 70–120), all three models show very similar behaviour. The characteristic bump is related to the inclusion of low-accuracy terrestrial data (in certain regions) in the EGM2008 model. Here, we can safely assume that the accuracy of all three GOCE models outperforms the EGM2008 model in this spectral range. This issue will be discussed in more detail in Sect. 6.

At around degree 120 the DIR solution starts to deviate significantly from the other two models, reflecting the impact of terrestrial gravity field data imported via the EIGEN-5C a priori model, which has been used in the DIR processing. The models TIM and SPW start to deviate slightly from each other at degrees 170–180. This is a result of the degree-selective Kaula regularization applied by TIM in the high degrees in order to improve the signal-to-noise ratio for the high degrees, while no explicit regularization was applied by SPW, where regularization only implicitly enters via the choice of the covariance function. Without applying regularization to the TIM solution, it would be very similar to the SPW result (compare with Fig. 10, red curve). For comparison, the light blue curve in Fig. 14 shows the deviations of the GRACE-only model ITG-Grace2010s from EGM2008.

In addition to the spectral comparisons in Fig. 14 we inspected the differences between the three GOCE models in the spatial domain. For this purpose we computed $1^\circ \times 1^\circ$ geoid height grids for the GOCE models and for EGM2008 and computed rms values of the differences between these four models between -80° and 80° latitude (i.e. excluding the polar caps). This has been done for the common degree range of the three GOCE models (degree 0–210) and for the medium-frequency range (degrees 70–120) where all three models show a very similar behaviour (cf. Fig. 14). The obtained numbers are given in Table 5 and can be summarized in the following:

Table 5 Rms values (m) of geoid height differences between in the three GOCE models and to EGM2008 for the common degree range of the GOCE models, i.e. degrees 0–210 (lower triangle) and for the degree range 70–120 (upper triangle)

	Degree range: 70–120			
	TIM	SPW	DIR	EGM2008
TIM	×	0.021	0.026	0.068
SPW	0.120	×	0.021	0.065
DIR	0.149	0.178	×	0.064
EGM2008	0.204	0.223	0.108	×
	Degree range: 0–210			

The rms values were computed from global $1^\circ \times 1^\circ$ grids excluding the polar caps (latitude range of -80° to 80°)

- When considering the whole common degree range (0–210) the TIM and the SPW solutions are closer than TIM resp. SPW and the DIR solution. In this case the DIR solution shows a stronger consistency with EGM2008 than the other GOCE models.
- For the medium-frequency range the difference among the three GOCE models is much smaller (rms = 0.021–0.026 m) than that compared with EGM2008 (rms= 0.064–0.068 m).

Thus, the findings from the spectral comparisons in Fig. 14 are in agreement with the differences among the three GOCE models in the spatial domain as given in Table 5.

Figure 15 displays the estimated standard deviations of the coefficients, representing the square root of the main diagonal elements of the variance–covariance matrix. Comparing the three solutions, it is obvious that they show a different scaling. The TIM (Fig. 15b) and SPW (Fig. 15c) error estimates show similar amplitudes, while the formal errors of DIR are significantly lower. The comparison of TIM and SPW with external gravity field information (GRACE-only and combined models) reveals that the gravity field errors and the corresponding statistical error estimates are consistent, while the DIR error estimates turn out to be too optimistic.

A closer look reveals that these error estimates show specific features of the processing rationale. While DIR and SPW show rather small errors in the low degrees, they are significantly larger in the TIM model, again reflecting the fact that kinematic orbits and no a-priori gravity field information have been used. Another striking fact is that DIR and SPW reflect almost an absence of the polar gap problem, i.e. bad estimates of the zonal and near-zonal coefficients due to the polar gaps. This is explained by the fact that these two models applied strong regularization by introducing a-priori gravity field information in the polar cap areas, either directly (DIR; cf. Sect. 4.1) or via the use of the Quick-look model (SPW, cf. Sect. 4.3).

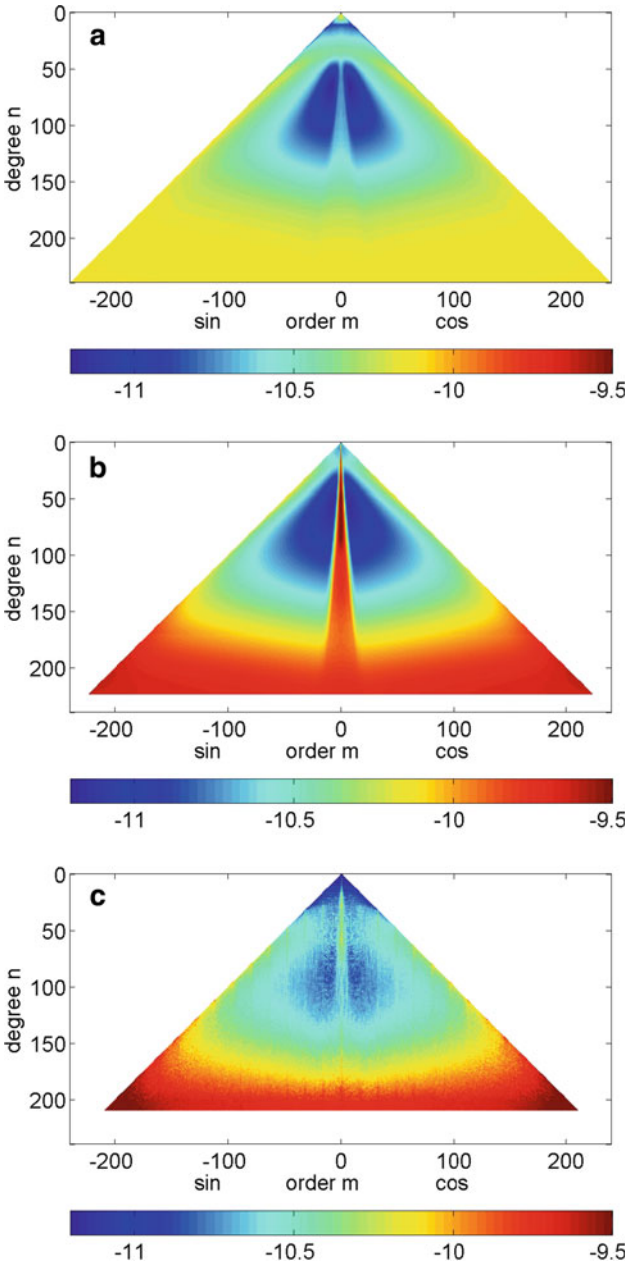

Fig. 15 Estimated coefficient standard deviations: **a** DIR; **b** TIM; **c** SPW. Scaling is $\log_{10}(|\cdots|)$

The rugged picture of the SPW model is due to the fact that the full variance–covariance matrix has been computed by Monte Carlo techniques with only 400 samples, while it is derived by a rigorous inversion of a full normal equation matrix in the case of DIR and TIM.

Comparing these error estimates to the deviations from an a priori model such as EGM2008 (cf. Fig. 14), it is evident that the TIM and SPW solutions show consistently a decreasing performance with increasing harmonic degree. In the DIR solution the differences to EGM2008 become smaller for high degrees, while the corresponding error esti-

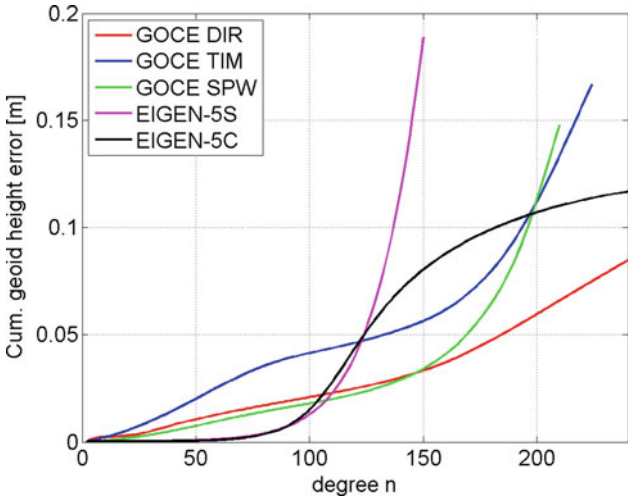

Fig. 16 Cumulative geoid height errors (m) of the three GOCE models DIR, TIM and SPW, and the EIGEN satellite-only and combined models EIGEN-5S and EIGEN-5C as a reference

mates increase. This also shows that the DIR solution is not independent from the chosen a priori gravity field.

Based on the error triangles displayed in Fig. 15, cumulative geoid height errors have been computed. The results are shown in Fig. 16, and reveal a very similar picture as already discussed above. The error estimates of the DIR solutions are generally lower. In the low degrees, the performance of the TIM model is inferior due to the fact that it is based on the kinematic GOCE orbits only. All three models outperform the GRACE-only model EIGEN-5S beyond degree 110. Beyond degree 180–190, combined models start to become superior, at least in those regions where high-quality terrestrial gravity field or satellite altimetry data are available (cf. Sect. 6).

Together with the coefficient solutions, also full variance–covariance matrices complete to degree/order 240 (DIR)/224 (TIM)/210 (SPW) are available. In order to prove the plausibility of these matrices, rigorous covariance propagation was performed to propagate the coefficient errors to geoid height errors on a global grid. Figure 17 shows the specific error structure of these fields, illustrating that the overall picture of the three models is the same. Please note that the colour scale of the DIR solution (Fig. 17a) is different in order to make it comparable with the other two models. The rugged structure of the SPW (Fig. 17c) model is again due to the fact that the underlying variance–covariance matrix was estimated by Monte Carlo techniques.

The zonal band structure with larger errors in the equatorial regions is due to the fact that a larger number of observations is measured at high latitudes, because of the meridian convergence, and thus the convergence of the satellite ground tracks. The asymmetry with respect to the equator and larger standard deviations in the southern hemisphere result from the orbit configuration, because the average satellite altitude is higher in this region, leading to a slightly increased attenuation of the gravity field signals at satellite height. The longitudinal striping structure is an expression of the data distribution (orbit ground tracks), because with a data volume of 71 days slightly more than one full repeat cycle of 61 days was included in the solution. Also the significantly degraded performance in the polar cap areas, where no observations are available, is expressed by the variance–covariance information.

6 Validation against reference gravity field information

The outcome of the GOCE gravity field processing as explained in Sect. 5 is the first GOCE gravity field model, given in three versions derived by the three different approaches. In this section, these new models are validated against existing gravity field models, deliberately using a variety of different reference models to obtain a representative picture.

One of the most remarkable characteristics of this new global satellite-only gravity field is the higher spatial resolution in comparison with the gravity field models based on the most recent gravity field mission GRACE and its precursor mission CHAMP. This can be seen in Fig. 18, where gravity anomalies over Europe, Western Asia and Northern Africa from the most recent CHAMP and GRACE gravity field models are given in comparison with the GOCE TIM model. The plots in this figure were computed with the respective maximum degrees of the three gravity field models.

For CHAMP the model AIUB-CHAMP03S (maximum degree 100) has been used in this study. This model, comprising 8 years of CHAMP data, has been computed with the so-called celestial mechanics approach (Beutler 2005; Beutler et al. 2010) and has a spatial resolution of about 200 km.

The gravity anomalies displayed in Fig. 18b are computed from the GRACE model ITG-Grace2010s (Mayer-Gürr et al. 2010b, maximum degree 180), which is based on 7 years of GRACE data processed by the so-called short arc integration method (Mayer-Gürr 2006; Mayer-Gürr et al. 2010a). The spatial resolution of ITG-Grace2010s is about 120 km. The spatial resolution of the GOCE model, which for this comparison is the one computed by the time-wise approach and has a maximum degree/order of 224, is about 80 km. The higher spatial resolution of the GOCE model w.r.t. the GRACE model is visible in Fig. 18c, for instance for the Arabian Peninsula, the Ural mountains and Western Siberia. For the region of Egypt and Sudan and for the Indian Ocean, a disappearance of north-south stripes is noticeable when comparing Fig. 18b, c, one must keep in mind that this GOCE

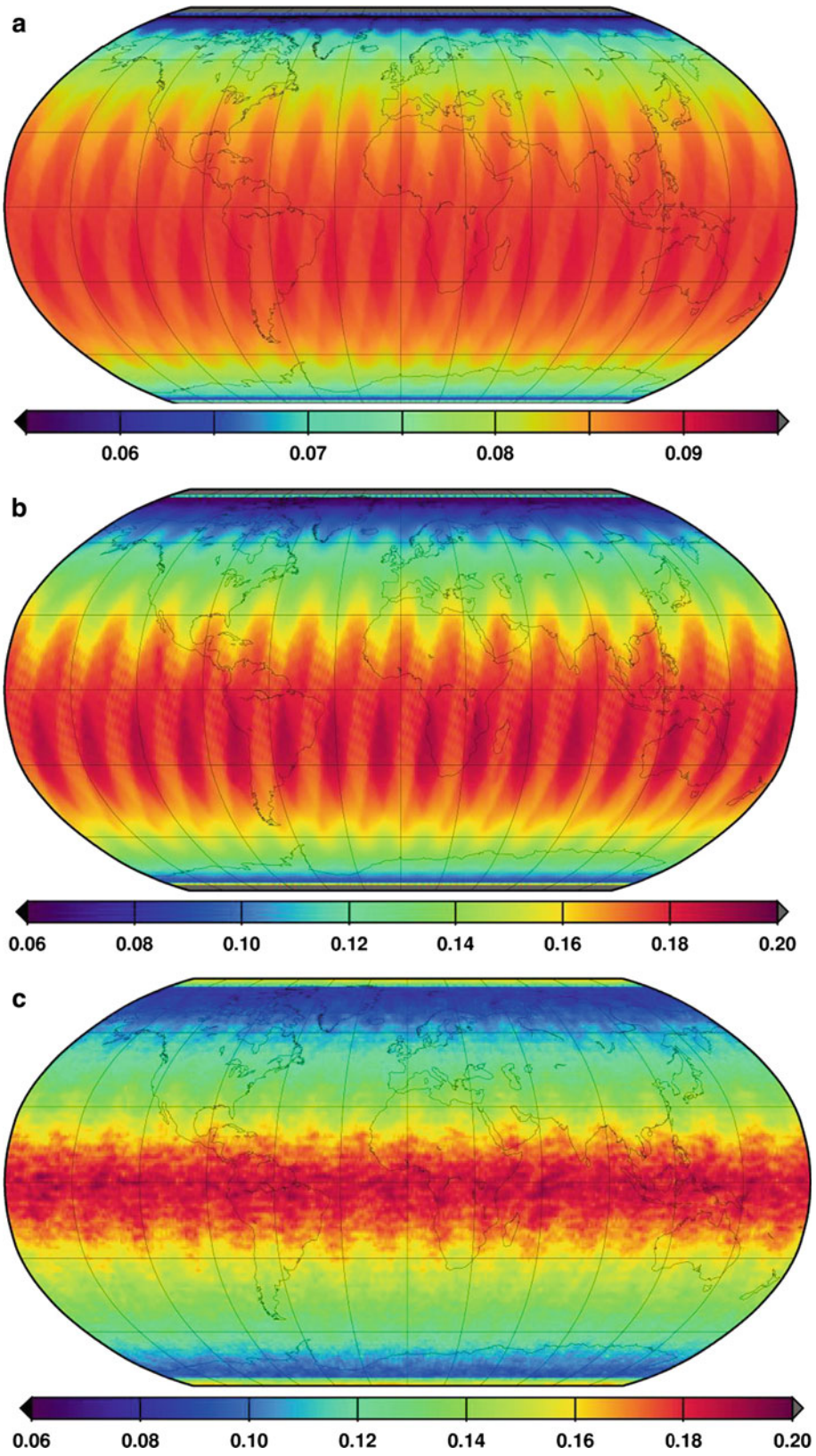

Fig. 17 Propagated geoid height errors (m): **a** DIR; **b** TIM; **c** SPW; please note the different scale of DIR compared with TIM and SPW

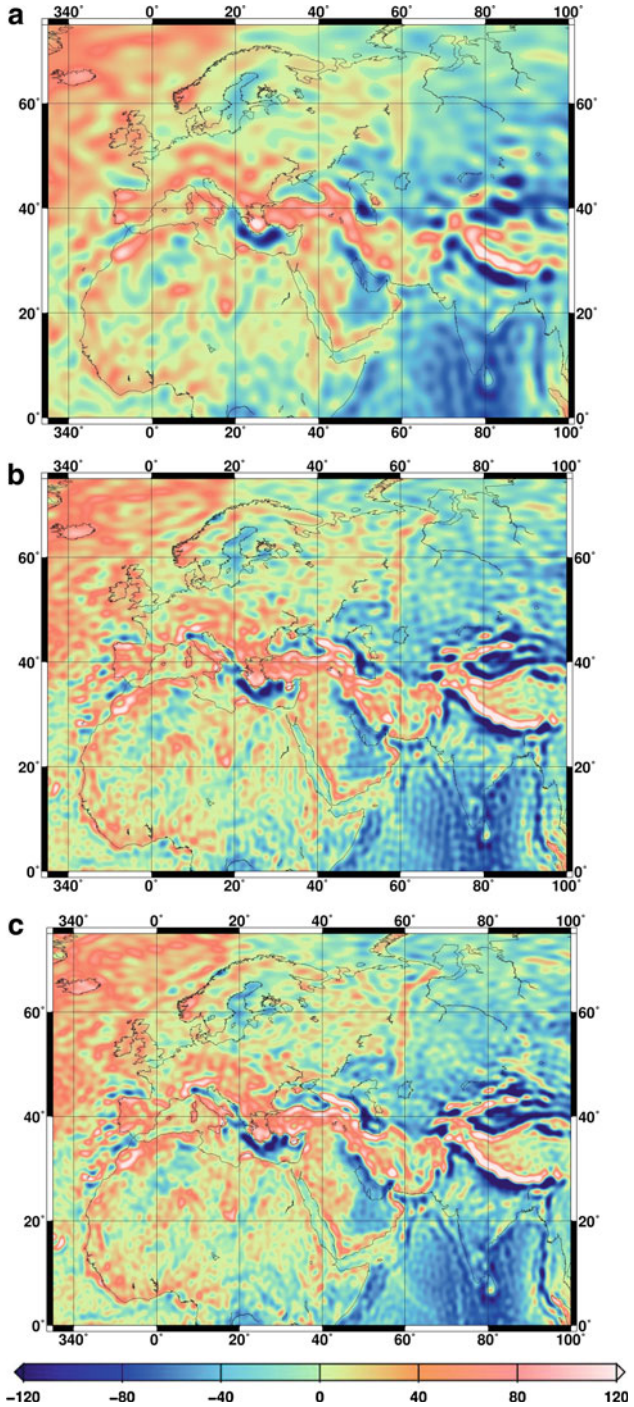

Fig. 18 Gravity anomalies over Europe, Western Asia and North Africa (mGal) from: **a** CHAMP (AIUB-CHAMP03S); **b** GRACE (ITG-Grace2010s); **c** GOCE (TIM)

model was obtained from only 2 months of data, while the GRACE model is based on more than 7 years of data.

The comparison of the first GOCE gravity field models with the most recent combined gravity field models gives further interesting and promising results concerning the potential of the GOCE mission. Figure 19 shows a comparison of the GOCE DIR model to EIGEN-5C (Förste et al. 2008b; Flechtner et al. 2010), which has been used as a priori gravity field for the data processing within the HPF. Figure 19a shows the geoid height error of EIGEN-5C obtained by rigorous error propagation from the full variance/covariance matrix up to spherical harmonic degree/order 260.

Figure 19b illustrates the patchwork of the terrestrial and altimetry data as used for EIGEN-5C. White areas indicate data gaps without available terrestrial data. These areas had been filled by a GRACE model. The contribution of the terrestrial data in the combined solution starts at spherical harmonic degree 70 (Förste et al. 2008a). Most of the used terrestrial data are newer data sets of known high quality and of spatial resolutions better than 0.5 degrees. But two gravity anomaly data sets (brown and light-blue) are relatively old data sets of only 0.5 degree resolution which were already incorporated in the EGM96 model (Lemoine et al. 1998), and which were published by the National Geospatial Intelligence Agency NGA (Kenyon and Pavlis 1997). For further details on the terrestrial data and the combination strategy of EIGEN-5C, see Förste et al. (2008a), and Shako et al. (2010).

Figure 19c shows the geoid height differences between GOCE and EIGEN-5C, resolved up to degree/order 240. From the comparison of the three sub-plots of Fig. 19 the following conclusion can be made:

- GOCE and EIGEN-5C show a high consistency for the oceans, for Europe, Northern Asia and North America. At this point it is important to emphasize that in these areas GOCE provides a pure high-resolution geoid, which is independent of altimetry (if no combined a priori model is used).
- For South America, Africa and Asia, the largest geoid height differences between GOCE and EIGEN-5C coincide with data gaps in terrestrial data and with regions of large geoid height errors in the error propagation.
- In Antarctica the propagated errors are not significantly larger (compared with the data gaps in the other continents), but the differences between GOCE and EIGEN-5C are in the order of 0.5 m or even larger. In contrast to this, the geoid height differences in Antarctica between GOCE and EGM2008 are considerably smaller (below 20 cm; see Fig. 20). It is known that EGM2008 contains no terrestrial data in Antarctica (Pavlis et al. 2008). Therefore, one can conclude that the NGA Antarctic gravity anomaly data as used in EIGEN-5C are of low quality and degrade the model to some degree. This data set should no longer be used in the future.
- The gravity anomaly data used for Western China seems to be also of low quality, since here the region of significant geoid height differences between GOCE and EIGEN-5C is larger than the extension of the data gaps.

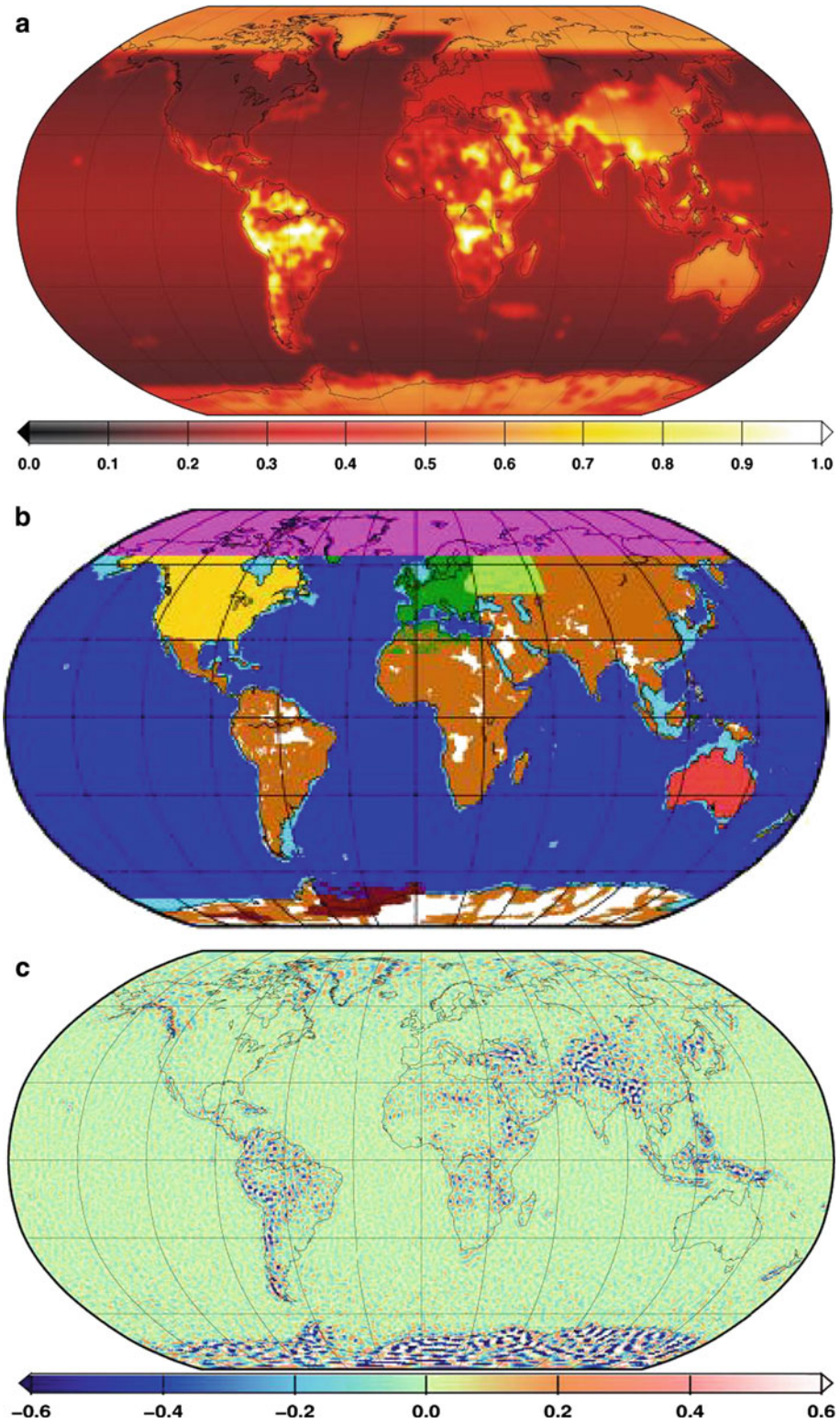

Fig. 19 Comparison of EIGEN-5C with the GOCE (DIR) model: **a** geoid height error (m) of EIGEN-5C obtained by rigorous error propagation from the full variance/covariance matrix up to degree/order 260; **b** patchwork of the terrestrial and altimetry data as used for EIGEN-5C; **c** geoid height differences (m) between GOCE and EIGEN-5C, up to degree/order 240

It should be noted that the pattern of low-quality terrestrial data in the geoid height differences between GOCE and combined models is also visible in the differences between the latest GRACE-only model ITG-Grace2010s and combined models (for example with EGM2008, see Fig. 21). Consequently, it is not a surprise that the geoid height differences between this GRACE-only and the GOCE models do not contain these signatures of low-quality terrestrial data

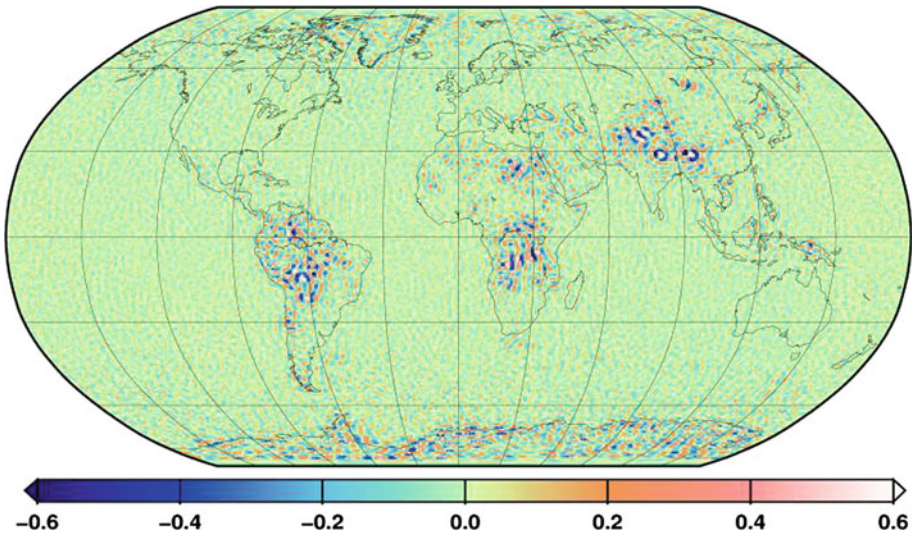

Fig. 20 Geoid height differences (m) between GOCE (DIR) and EGM2008 up to degree/order 240

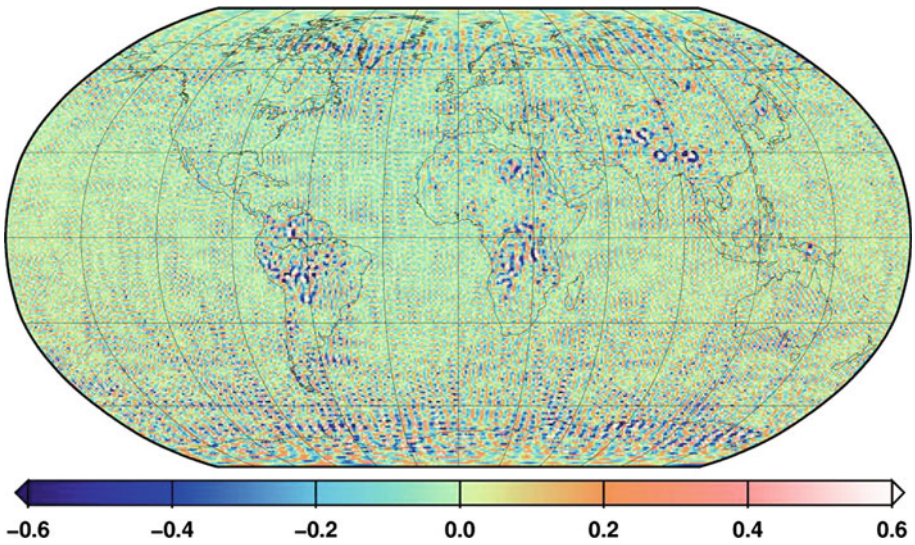

Fig. 21 Geoid height differences (m) between ITG-Grace2010s and EGM2008 up to degree/order 180

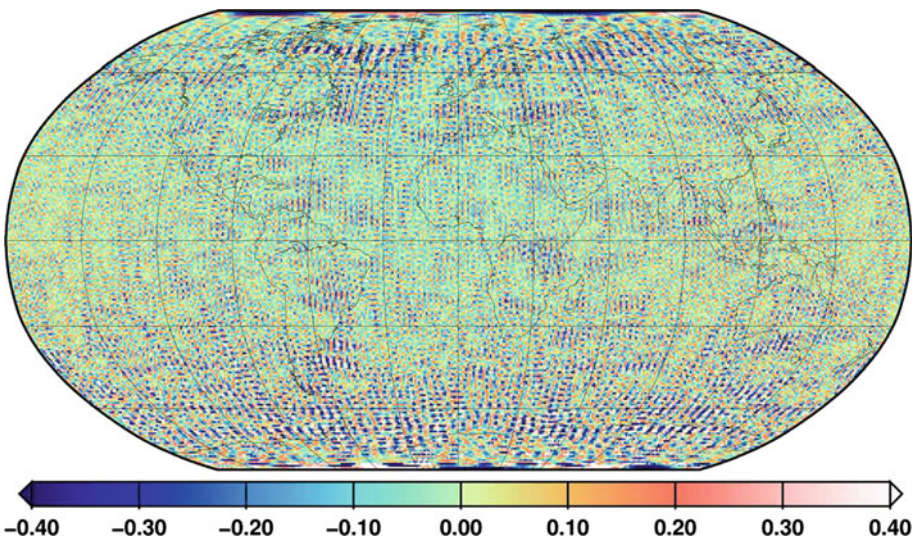

Fig. 22 Geoid height differences (m) between ITG-Grace2010s and GOCE (SPW) up to degree/order 180

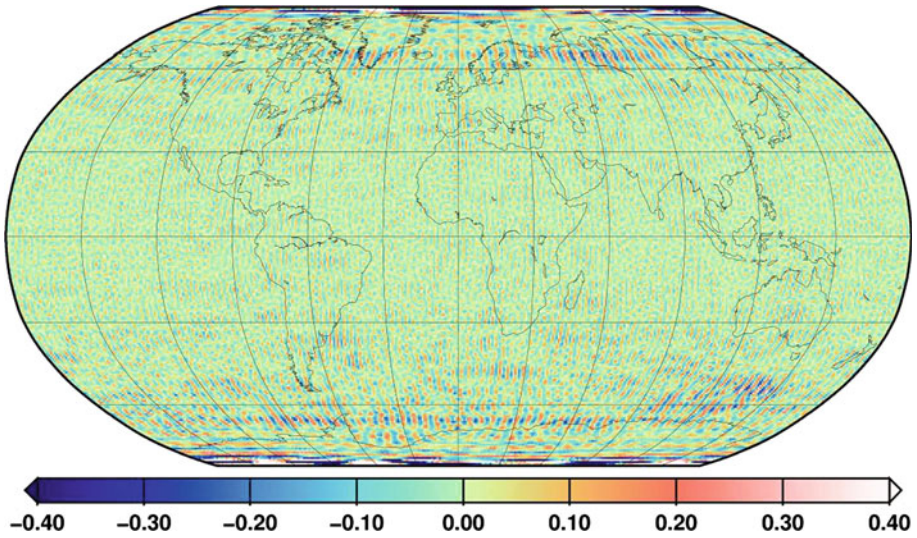

Fig. 23 Geoid height differences (m) between ITG-Grace2010s and GOCE (TIM) for the spherical harmonic degree range 80–160

(see Fig. 22; please note the different scales of the Figs. 21 and 22). But this pattern of low-quality terrestrial data is much more pronounced in the case of the GOCE models, since the short wavelengths of the GRACE model are still suffering from the well-known meridian stripes, which are apparent here in Figs. 22 and 23.

A further comparison between GRACE and the GOCE models can be deduced from Fig. 14. They show a similar spectral behaviour between degree 80 and 160. This can be interpreted as a confirmation of the GOCE models by GRACE for these spherical harmonic degrees. This finding corresponds to the spatial distribution of the geoid height differences between GOCE (TIM) and ITG-Grace2010s which were computed only from the spherical harmonic coefficients between degrees 80 and 160 (Fig. 23). Apart from the GOCE polar gaps and a remaining GRACE striping pattern these geoid height differences are small and have a very homogenous spatial distribution. This means that the comparison of the first GOCE models with GRACE highlights a high consistency of these gravity field models for the spherical harmonic degree range 80–160.

One of the most important results of the comparison of the first GOCE models with recent combined gravity field models is the discovery of the occurrence of low-quality terrestrial data in the combined models EIGEN-5C and EGM2008 for some regions. Vice versa, this finding indicates the expected high spatial resolution of GOCE.

A further validation of the three gravity field models by means of orbit residuals and using independent GPS/leveling observations is performed by Gruber et al. (2011).

First investigations concerning the derivation of dynamic ocean topography based on GOCE-only models demonstrate that they outperform GRACE gravity fields (Bingham et al. 2011).

7 Conclusions and outlook

Three independent and complementary solution strategies for the computation of global gravity models from 71 days of GOCE data have been presented. They are based on different rationales. In the direct method, based on the reference gravity field model EIGEN-5C, GOCE data are included to extend and further improve this a priori gravity field knowledge. In contrast, the philosophy of the time-wise approach is to produce a GOCE-only model in a rigorous sense, i.e. no external gravity field information is included, and thus the solution is solely based on GOCE data. The philosophy of the space-wise method is similar, but still a priori knowledge (EGM2008) was included in the low degrees, and the GOCE Quick-look model was used for data reduction and to set up the signal covariance model.

Due to the fact that the models are based on different processing philosophies, especially concerning the use of prior information and filtering strategies, they cannot and should not be compared directly. Therefore, which of the models to be used depends on the specific application. The time-wise solution is inferred from GOCE data exclusively. So, it is representative of the GOCE mission performance and constitutes an independent means of comparison with other global models, terrestrial gravity field data, and subsequently for a consistent combination with these complementary data types. In ocean regions it provides a pure high-resolution geoid being independent of altimetry, which will be beneficial for oceanography and the derivation of dynamic ocean topography. Since the time-wise solution is based only on 2 months of kinematic orbit data, it should not be used if the application requires best possible gravity field information in the low-harmonic degrees, because this must come from GRACE. In these spectral regions the direct and the space-wise models, which are using GRACE prior information, will

be superior, which is also reflected in orbit tests as part of the validation activities (Gruber et al. 2011). Additionally, due to the fact that a combined gravity field model has been used in the direct approach as a background and prior model, in a comparison with terrestrial gravity field data in well-surveyed areas this model will outperform the time-wise and the space-wise models in the high degrees starting at degree 150 (Gruber et al. 2011). The space-wise model is indeed an intermediate solution in the sense that it takes advantage of GRACE information at very low degrees and in the polar areas, but it is independent from external data at high degrees, where the contribution of GOCE is expected to be more significant.

In spite of these different approaches, when comparing the three GOCE solutions to existing satellite-only and combined gravity field models the main conclusions are quite similar and consistent, as has been discussed in Sect. 6. The actually achieved gravity field accuracy of these 2-month GOCE solution is estimated to be in the order of 10 cm in terms of geoid heights, and 3 mGal in terms of gravity anomalies, at a resolution of degree/order 200. A projection to the full nominal mission period (∼18 months) yields predictions of about 3 cm / 1 mGal, which is quite close to the original performance requirements. The main reason of the slightly inferior performance compared with the original specification is the actual gradiometer performance. At this point it does not quite meet the planned baseline inside the MBW. This is particularly true for the radial gradiometric component V_{ZZ} (cf. Fig. 3). The reason is not yet understood. Even if assuming that the current gradiometer performance cannot be substantially improved in the future, e.g. by modifications in the data pre-processing, the operation of the extended mission phase until end of 2012 will allow us to come close to the ambitious original performance specifications.

Acknowledgments The authors acknowledge the European Space Agency for the provision of the GOCE data. Significant parts of the work described in this manuscript are financed through European Space Agency contract no. 18308/04/NL/MM for the design, development and operation of the GOCE Level 2 data processing system. Parts of this work were financially supported by the BMBF Geotechnologien program REAL-GOCE, the Austrian Space Application Programme of FFG charged by BMVIT, and the Groupe de Recherche de Géodésie Spatiale (GRGS). Parts of the computations were performed at the Leibniz-Rechenzentrum of the Bavarian Academy of Sciences and on the JUROPA supercomputer at FZ Jülich. The computing time was granted by John von Neumann Institute for Computing (project HBN15). We also acknowledge the valuable comments by C.K. Shum and two other anonymous reviewers.

References

Albertella A, Migliaccio F, Reguzzoni M, Sansò F (2004) Wiener filters and collocation in satellite gradiometry. In: Sansò F (ed) International Association of Geodesy Symposia, "V Hotine-Marussi Symposium on Mathematical Geodesy", vol 127, 17–21 June 2002, Matera, Italy. Springer, Berlin, pp 32–38

Andersen OA, Knudsen P (2009) DNSC08 mean sea surface and mean dynamic topography models. J Geophys Res 114. doi:10.1029/2008JC005179

Badura T (2006) Gravity field analysis from satellite orbit information applying the energy integral approach. Dissertation, Graz University of Technology

Beutler G (2005) Methods of celestial mechanics. Physical, mathematical, and numerical principles, vol I. Springer. ISBN:978-3-540-40749-2

Beutler G, Jäggi A, Mervart L, Meyer U (2010) The celestial mechanics approach—theoretical foundations. J Geod 84(10):605–624. doi:10.1007/s00190-010-0401-7

Biancale R, Balmino G, Lemoine J-M, Marty J-C, Moynot B, Barlier F, Exertier P, Laurain O, Gegout P, Schwintzer P, Reigber C, Bode A, Gruber T, König R, Massmann F-H, Raimondo JC, Schmidt R, Zhu SY (2000) A new global Earth's gravity field model from satellite orbit perturbations: GRIM5-S1. Geophys Res Lett 27(22):3611–3614

Bingham RJ, Knudsen P, Andersen O, Pail R (2011) An initial estimate of the North Atlantic steady-state geostrophic circulation from GOCE. Geophys Res Lett 38:1. doi:10.1029/2010GL045633

Bock H, Jäggi A, Meyer U, Visser P, van den Ijssel J, van Helleputte T, Heinze M, Hugentobler U (2011) GPS-derived orbits for the GOCE satellite. J Geod (submitted)

Bouman J, Fiorot S, Fuchs M, Gruber T, Rispens S, Schrama E, Tscherning C, Veicherts M, Visser P (2011) GOCE gravity gradients along the orbit. J Geod. doi:10.1007/s00190-011-0464-0

Boxhammer CH, Schuh W-D (2006) GOCE gravity field modeling: computational aspects—free kite numbering scheme. In: Rummel R (ed) et al Observation of the Earth system from Space. Springer, Berlin, pp 209–224

Brockmann JM, Kargoll B, Krasbutter I, Schuh W-D, Wermuth M (2010) GOCE data analysis: from calibrated measurements to the global Earth gravity field. In: Flechtner et al (eds) System Earth via geodetic-geophysical space techniques. Springer, New York, pp 213–229. ISBN 978-3-642-10227-1. doi:10.1007/978-3-642-10228-8_17

Bruinsma SL, Marty JC, Balmino G, Biancale R, Förste C, Abrikosov O, Neumayer H (2010) GOCE gravity field recovery by means of the direct numerical method. In: Lacoste-Francis H (ed) Proceedings of the ESA living planet symposium, ESA Publication SP-686. ESA/ESTEC. ISBN:978-92-9221-250-6; ISSN: 1609-042X

Colombo OL (1981) Numerical methods for harmonic analysis on the sphere. Report No. 310, Department of Geodetic Science and Surveying, The Ohio State University, Columbus, Ohio

Drinkwater MR, Floberghagen R, Haagmans R, Muzi D, Popescu A (2003) GOCE: ESA's first Earth explorer core mission. In: Beutler et al (eds) Earth gravity field from Space—from sensors to Earth Science, Space Sciences Series of ISSI, vol 18. Kluwer, Dordrecht, pp 419–432. ISBN:1-4020-1408-2

EGG-C (2010a) GOCE Level 2 Product Data Handbook. GO-MA-HPF-GS-0110, Issue 4.2. European Space Agency, Noordwijk. http://earth.esa.int/pub/ESA_DOC/GOCE/Product_Data_Handbook_4.1.pdf

EGG-C (2010b) GOCE Standards. GP-TN-HPF-GS-0111, Issue 3.2. European Space Agency, Noordwijk. http://earth.esa.int/pub/ESA_DOC/GOCE/GOCE_Standards_3.2.pdf

Flechtner F, Dahle C, Neumayer KH, König R, Förste C (2010) The Release 04 CHAMP and GRACE EIGEN gravity field models. In: Flechtner et al (eds) System Earth via geodetic-geophysical space techniques. Springer, New York, pp 41–58. ISBN:978-3-642-10227-1. doi:10.1007/978-3-642-10228-8_4

Förste C, Schmidt R, Stubenvoll R, Flechtner F, Meyer U, König R, Neumayer H, Biancale R, Lemoine JM, Bruinsma S, Loyer S, Barthelmes F, Esselborn S (2008) The GeoForschungsZentrum Potsdam/Groupe de Recherche de Gèodésie Spatiale satellite-only and combined gravity field models: EIGEN-GL04S1 and EIGEN-GL04C. J Geod 82:331–346. doi:10.1007/s00190-007-0183-8

Förste C, Flechtner F, Schmidt R, Stubenvoll R, Rothacher M, Kusche J, Neumayer KH, Biancale R, Lemoine JM, Barthelmes F, Bruinsma S, Koenig R, Meyer U (2008b) EIGEN-GL05C—a new global combined high-resolution GRACE-based gravity field model of the GFZ-GRGS cooperation. General Assembly European Geosciences Union (Vienna, Austria 2008), Geophys Res Abstr 10, Abstract No. EGU2008-A-06944

Gruber T (2009) Evaluation of the EGM2008 gravity field by means of GPS-levelling and sea surface topography solutions; External quality evaluation reports of EGM08. Newton's Bull 4:3–17. Bureau Gravimétrique International (BGI)/International Geoid Service (IGeS). ISSN:1810–8555

Gruber T, Visser P, Ackermann C, Hosse M (2011) Validation of GOCE gravity field models by means of orbit residuals and geoid comparisons. J Geod (submitted)

Ilk K-H, Löcher A (2005): The Use of Energy Balance Relations for Validation of Gravity Field Models and Orbit Determination Results. International Association of Geodesy Symposia, 2005, Vol. 128, Symposium G04, 494-499, doi:10.1007/3-540-27432-4_84

Jäggi A, Beutler G, Meyer U, Prange L, Dach R, Mervart L (2009) AIUB-GRACE02S—status of GRACE gravity field recovery using the celestial mechanics approach. In: Paper presented at the IAG Scientific Assembly 2009, Aug 31–Sept 4, 2009, Buenos Aires, Argentina

Jäggi A, Bock H, Prange L, Meyer U, Beutler G (2010) GPS-only gravity field recovery with GOCE, CHAMP, and GRACE. Adv Space Res 47(6):1020–1028. doi:10.1016/j.asr.2010.11.008

Jekeli C (1999) The determination of gravitational potential differences from satellite-to-satellite tracking. Celest Mech Dyn Astron 75:85–101

Kenyon SC, Pavlis NK (1997) The development of a global surface gravity data base to be used in the joint DMA/GSFC geopotential model. In: Segawa J, Fujimoto H, Okubo S (eds) Gravity, geoid and marine geodesy. IAG symposia, vol 117. Springer, Heidelberg, pp 470–477

Koch KH, Kusche J (2002) Regularization of geopotential determination from satellite data by variance components. J Geod 76:259–268. doi:10.1007/s00190-002-0245-x

Lemoine FG, Kenyon SC, Factor JK, Trimmer RG, Pavlis NK, Chinn DS, Cox CM, Klosko SM, Luthcke SB, Torrence MH,Wang YM, Williamson RG, Pavlis EC, Rapp RH, Olsen TR (1998) The development of the joint NASA GSFC and the National Imagery and Mapping Agency (NIMA) geopotential model EGM96. NASA technical paper NASA/TP-1998-206861. Goddard Space Flight Center, Greenbelt

Marty J, Bruinsma, Balmino G, Abrikosov O, Förste C, Rothacher M (2005) Gravity field recovery with simulated GOCE observations. American Geophysical Union, Fall Meeting 2005, abstract #G33C-0052

Mayer-Gürr T (2006) Gravitationsfeldbestimmung aus der Analyse kurzer Bahnbögen am Beispiel der Satellitenmissionen CHAMP und GRACE. Dissertation, University of Bonn

Mayer-Gürr T, Ilk KH, Eicker A, Feuchtinger M (2005) ITG-CHAMP01: a CHAMP gravitiy field model from short kinematical arcs of a one-year observation period. J Geod 78(7–8). doi:10.1007/s00190-004-0413-2

Mayer-Gürr T, Eicker A, Kurtenbach E, Ilk KH (2010a) ITG-GRACE: global static and temporal gravity field models from GRACE data. In: Flechtner et al. (eds) System Earth via geodetic-geophysical space techniques. Springer, New York. ISBN:978-3-642-10227-1. doi:10.1007/978-3-642-10228-8_13

Mayer-Gürr T, Kurtenbach E, Eicker A (2010b) The satellite-only gravity field model ITG-Grace2010s. http://www.igg.uni-bonn.de/apmg/index.php?id=itg-grace2010

Mayrhofer R, Pail R, Fecher T (2010) Quick-look gravity field solution as part of the GOCE quality assessment. In: Lacoste-Francis H (ed) Proceedings of the ESA living planet symposium. ESA Publication SP-686, ESA/ESTEC. ISBN:978-92-9221-250-6;ISSN:1609-042X

Metzler B, Pail R (2005) GOCE data processing: the spherical cap regularization approach. Stud Geophys Geod 49:441–462. doi:10.1007/s11200-005-0021-5

Migliaccio F, Reguzzoni M, Sansò F (2004) Space-wise approach to satellite gravity field determination in the presence of coloured noise. J Geod 78:304–313. doi:10.1007/s00190-004-0396-z

Migliaccio F, Reguzzoni M, Sansò F, Tselfes N (2007) On the use of gridded data to estimate potential coefficients. In: Proceedings 3rd GOCE user workshop, Frascati, ESRIN, November 2006, ESA SP-627. European Space Agency, Noordwijk, pp 311–318. ISBN:92-9092-938-3; ISSN:1609-042X

Migliaccio F, Reguzzoni M, Sansò F, Tselfes N (2009) An error model for the GOCE space-wise solution by Monte Carlo methods. In: Sideris MG (ed) IAG symposia, "Observing our Changing Earth", vol 133. Springer, Berlin, pp 337–344. doi:10.1007/978-3-540-85426-5

Migliaccio F, Reguzzoni M, Sansò F, Tscherning CC, Veicherts M (2010a) GOCE data analysis: the space-wise approach and the first space-wise gravity field model. In: Lacoste-Francis H (ed) Proceedings of the ESA living planet symposium. ESA Publication SP-686, ESA/ESTEC. ISBN:978-92-9221-250-6; ISSN:1609-042X

Migliaccio F, Reguzzoni M, Tselfes N (2010b) A simulated space-wise solution using GOCE kinematic orbits. Bull Geod Geomat 1:55–68

Moritz H (1989) Advanced physical geodesy, 2nd edn. Wichmann Verlag, Karlsruhe

Oppenheim AV, Schafer RW (1999) Zeitdiskrete Signalverarbeitung. 3. Auflage. Oldenbourg Verlag, München Wien

Pail R (2005) A parametric study on the impact of satellite attitude errors on GOCE gravity field recovery. J Geod 79:231–241. doi:10.1007/s00190-005-0464-z

Pail R, Plank G (2002) Assessment of three numerical solution strategies for gravity field recovery from GOCE satellite gravity gradiometry implemented on a parallel platform. J Geod 76:462–474. doi:10.1007/s00190-002-0277-2

Pail R, Metzler B, Lackner B, Preimesberger T, Höck E, Schuh WD, Alkathib H, Boxhammer Ch, Siemes Ch, Wermuth M (2007a) GOCE gravity field analysis in the framework of HPF: operational software system and simulation results. In: Proceedings 3rd GOCE user workshop, Frascati, ESRIN, November 2006, ESA SP-627. European Space Agency, Noordwijk, pp 249–256

Pail R, Metzler B, Preimesberger T, Lackner B, Wermuth M (2007b) GOCE quick-look gravity field analysis in the framework of HPF. In: Proceedings 3rd GOCE user workshop, Frascati, ESRIN, November 2006, ESA SP-627. European Space Agency, Noordwijk, pp 325–332

Pail R, Goiginger H, Mayrhofer R, Schuh WD, Brockmann JM, Krasbutter I, Höck E, Fecher T (2010) Global gravity field model derived from orbit and gradiometry data applying the time-wise method. In: Lacoste-Francis H (ed) Proceedings of the ESA living planet symposium. ESA Publication SP-686, ESA/ESTEC. ISBN:978-92-9221-250-6; ISSN:1609-042X

Papoulis A (1984) Signal analysis. McGraw Hill, New York

Pavlis NK, Holmes SA, Kenyon SC, Factor JK (2008) An Earth gravitational model to degree 2160: EGM2008. In: Paper presented at

the 2008 General Assembly of the European Geosciences Union, Vienna, Austria, April 13–18, 2008

Reguzzoni M, Tselfes N (2009) Optimal multi-step collocation: application to the space-wise approach for GOCE data analysis. J Geod 83:13–29. doi:10.1007/s00190-008-0225-x

Reigber Ch, Balmino G, Schwintzer P, Biancale R, Bode A, Lemoine JM, Koenig R, Loyer S, Neumayer H, Marty JC, Barthelmes F, Perosanz F (2002) A high quality global gravity field model from CHAMP GPS tracking data and accelerometry (EIGEN-1S). Geophys Res Lett 29:14. doi:10.1029/2002GL015064

Reigber C, Jochmann H, Wünsch J, Neumayer KH, Schwintzer P (2003) First insight into temporal gravity variability from CHAMP. In: Reigber C, Lühr H, Schwintzer P (eds) First CHAMP mission results for gravity, magnetic and atmospheric studies. Springer, New York, pp 128–133

Rummel R, van Gelderen M, Koop R, Schrama E, Sansó F, Brovelli M, Miggliaccio F, Sacerdote F (1993) Spherical harmonic analysis of satellite gradiometry. Neth Geod Comm, Publications on Geodesy, vol 39, Delft, The Netherlands

Rummel R, Gruber T, Koop R (2004) High level processing facility for GOCE: products and processing strategy. In: Lacoste H (ed) Proceedings of the 2nd international GOCE user workshop "GOCE, The Geoid and Oceanography". ESA SP-569, ESA. ISBN:92-9092-880-8; ISSN:1609-042X

Schuh WD (1996) Tailored numerical solution strategies for the global determination of the Earth's gravity field. Mitteil Geod Inst TU Graz, no 81, 156 pp

Schuh WD (2002) Improved modelling of SGG-data sets by advanced filter strategies. ESA-Project "From Eötvös to mGal+". Final report, ESA/ESTEC Contract 14287/00/NL/DC, WP 2. ESA, Noordwijk, pp 113–181

Schuh WD, Boxhammer C, Siemes C (2006) Correlations, variances, covariances—from GOCE signals to GOCE products. In: Proceedings 3rd GOCE user workshop, Frascati, ESRIN, November 2006. ESA SP-627, European Space Agency, Noordwijk, pp 257–264

Schuh WD, Brockmann JM, Kargoll B, Krasbutter I, Pail R (2010) Refinement of the stochastic model of GOCE scientific data and its effect on the in-situ gravity field solution. In: Proceedings of the ESA living planet symposium, 28 June–2 July 2010, Bergen, Norway

Shako R, Förste C, Abrikosov O, Kusche J (2010) GOCE and its use for a high-resolution global gravity combination model. In: Flechtner F et al (eds) System Earth via geodetic-geophysical space techniques. Springer, New York, pp 231–242. ISBN:978-3-642-10227-1; ISBN:978-3-642-10228-8

Siemes C (2008) Digital Filtering algorithms for decorrelation within large least squares problems. Dissertation, University of Bonn

Sneeuw N (2000) A semi-analytical approach to gravity field analysis from satellite observations. DGK, C:527, Verlag der Bayerischen Akademie der Wissenschaften. ISBN:3-7696-9566-6; ISSN:0065-5325

Sneeuw N, van Gelderen M (1997) The polar gap. In: Geodetic boundary value problems in view of the one centimeter geoid. Lecture notes in Earth Sciences, vol 65. Springer, Berlin, pp 559–568. doi:10.1007/BFb0011699

Tapley BD, Bettadpur S, Watkins M, Reigber C (2004) The gravity recovery and climate experiment: mission overview and early results. Geophys Res Lett 31(9):L09607. American Geophysical Union. doi:10.1029/2004GL019920

Tapley B, Ries J, Bettadpur S, Chambers D, Cheng M, Condi F, Poole S (2007) The GGM03 mean Earth gravity model from GRACE. Eos Trans, AGU, 88(52). Fall Meet Suppl, Abstract G42A-03

Tscherning CC (2001) Computation of spherical harmonic coefficients and their error estimates using least squares collocation. J Geod 75:12–18. doi:10.1007/s001900000150

Visser PNAM, Sneeuw N, Gerlach C (2003) Energy integral method for gravity field determination from satellite orbit coordinates. J Geod 77:207–216. doi:10.1007/s00190-003-0315-8